



Long-term validation of MIPAS ESA operational products using MIPAS-B measurements

Gerald Wetzel¹, Michael Höpfner¹, Hermann Oelhaf¹, Felix Friedl-Vallon¹, Anne Kleinert¹, Guido Maucher¹, Miriam Sinnhuber¹, Janna Abalichin², Angelika Dehn³, and Piera Raspollini⁴

5 ¹Karlsruhe Institute of Technology, Institute of Meteorology and Climate Research, Karlsruhe, Germany

²Freie Universität Berlin, Institute of Meteorology, Berlin, Germany

³European Space Agency (ESA-ESRIN), Frascati, Italy

⁴Istituto di Fisica Applicata “N. Carrara” (IFAC) del Consiglio Nazionale delle Ricerche (CNR), Firenze, Italy

Correspondence to: Gerald Wetzel (gerald.wetzel@kit.edu)

10

Abstract

The Michelson Interferometer for Passive Atmospheric Sounding (MIPAS) was a limb-viewing infrared Fourier transform spectrometer that operated from 2002 to 2012 aboard the Environmental Satellite (ENVISAT). The final re-processing of the full MIPAS mission Level
15 2 data was performed with the ESA operational version 8 (v8) processor. This MIPAS data set not only includes retrieval results of pressure-temperature and the standard species H₂O, O₃, HNO₃, CH₄, N₂O, and NO₂, but also vertical profiles of volume mixing ratios of the more difficult to retrieve molecules N₂O₅, ClONO₂, CFC-11, CFC-12 (included since v6 processing), HCFC-22, CCl₄, CF₄, COF₂, and HCN (included since v7 processing). Finally, vertical profiles
20 of the species C₂H₂, C₂H₆, COCl₂, OCS, CH₃Cl, and HDO were additionally retrieved by the v8 processor.

The balloon-borne limb-emission sounder MIPAS-B was a precursor of the MIPAS satellite instrument. Several flights with MIPAS-B have been carried out during the 10 years operational phase of ENVISAT at different latitudes and seasons, including both operational periods where
25 MIPAS measured with full spectral resolution (FR mode) and with optimized spectral resolution (OR mode). All MIPAS operational products (except HDO) were compared to results inferred from dedicated validation limb sequences of MIPAS-B. To enhance the statistics of vertical profile comparisons, a trajectory match method has been applied to search for MIPAS coincidences along 2-day forward/backward trajectories running from the MIPAS-B
30 measurement geolocations. This study gives an overview of the validation results based on the



ESA operational v8 data comprising the MIPAS FR and OR observation periods. This includes an assessment of the data agreement of both sensors taking into account combined errors of the instruments. The difference between retrieved temperature profiles of both MIPAS instruments generally stays within ± 2 K in the stratosphere. For most gases, namely H₂O, O₃, HNO₃, CH₄,
35 N₂O, NO₂, N₂O₅, ClONO₂, CFC-11, CFC-12, HCFC-22, CCl₄, CF₄, COF₂, and HCN we find a 5 % to 20 % agreement of the retrieved vertical profiles of both MIPAS instruments in the lower stratosphere. For the species C₂H₂, C₂H₆, COCl₂, OCS, and CH₃Cl, however, larger differences within 20 % and 50 % appear in this altitude range.

40 1 Introduction

Satellite measurements of stratospheric trace gases are essential for monitoring the distribution and trend of these species on a global scale (Hegglin et al., 2021). The Environmental Satellite (ENVISAT) of the European Space Agency (ESA) operated ten years between 2002 and 2012. The Michelson Interferometer for Passive Atmospheric Sounding (MIPAS; Fischer et al., 2008)
45 was one of three chemistry instruments aboard ENVISAT, besides the Scanning Imaging Absorption Spectrometer for Atmospheric Chartography (SCIAMACHY; Bovensmann et al., 1999) and the Global Ozone Monitoring by Occultation of Stars (GOMOS) instrument (Bertaux et al., 1991). Validating instruments like MIPAS for the purpose of assessing measurement accuracy is an essential task. Stratospheric balloon measurements are particularly suitable to
50 reach this goal since these instruments are able to sound the atmosphere with high vertical resolution (e.g. Cortesi et al., 2007; Ridolfi et al., 2007; Wang et al., 2007; Wetzel et al., 2007; Payan et al., 2009; Wetzel et al., 2013a). The main logistical issue that the satellite and the validating balloon instruments observe the same air masses has to be considered carefully when performing balloon campaigns. Two principal comparison methods are common: (1) direct
55 matches where the balloon instrument measures at the same time and location where the satellite observation takes place and (2) trajectory matches where forward and backward trajectories are calculated from the balloon measurement geolocation to search for appropriate satellite overpasses. Several flights with the balloon version of MIPAS (Friedl-Vallon et al., 2004) were carried out during the operational time of ENVISAT. This study presents an overview of 10
60 years of MIPAS observations based on the recent ESA processor version 8 (v8; released in 2021; ESA, 2021; Dinelli et al., 2021) and provides the evaluation of the long-term performance of MIPAS covering the complete set of atmospheric parameters (except HDO) that have been



processed with the newest operational data version. In the following sections, validation activities, data analysis and validation results are described in detail.

65

2 Instruments and data analysis

2.1 MIPAS operations and data version

The limb-viewing Fourier transform spectrometer MIPAS on ENVISAT (hereinafter also referred to as MIPAS-E to better distinguish from the balloon instrument MIPAS-B) has been
70 designed to operate in the mid-infrared spectral region covering five spectral bands between 685 and 2410 cm^{-1} with a maximum optical path difference (MOPD) of 20 cm, equivalent to an unapodized full spectral resolution of 0.025 cm^{-1} (Fischer et al., 2008). The vertical instantaneous field of view (IFOV) was about 3 km. ENVISAT was launched into its sun-synchronous orbit by ESA on 1 March 2002 with 14.3 orbits/day and an Equator crossing local
75 solar time 10:00 (descending node). After the commissioning phase, MIPAS was run predominantly in its nominal measurement mode with full spectral resolution (called FR mode) from July 2002 until the end of March 2004. During each orbit approximately 72 limb scans covering tangent altitudes between 8 and 68 km were recorded (in steps of 3 km below 45 km) in the FR mode. The majority of validation studies based on correlative measurements
80 published so far were addressing MIPAS data recorded during this first time period. These measurements were originally reprocessed by the ESA Instrument Processing Facilities (IPF) v4.1 and v4.2, based on the Optimized Retrieval Model (ORM) code described in Ridolfi et al. (2000) and Raspollini et al. (2006), and covered pressure-temperature and the six constituents O_3 , H_2O , CH_4 , N_2O , HNO_3 , and NO_2 . The validation studies addressed these parameters and
85 constituents: pressure-temperature (Ridolfi et al., 2007), O_3 (Cortesi et al., 2007), HNO_3 (Wang et al., 2007), NO_2 (Wetzel et al., 2007), N_2O and CH_4 (Payan et al., 2009), and H_2O (Wetzel et al., 2013a).

After an increasing frequency of problems with the interferometer drive system in late 2003 and beginning of 2004 and upon subsequent detailed investigations it was decided to suspend
90 the nominal operations from March 2004 onwards for detailed investigations. From January 2005 onwards, the instrument was back to operation but at reduced MOPD (41 % of nominal) while maintaining the interferogram scan speed. During data processing, the interferograms were truncated to 8 cm MOPD, resulting in an unapodized spectral resolution of 0.0625 cm^{-1} .



95 The shorter acquisition time per interferogram led to the benefit of an equivalent improvement
in the vertical and horizontal (along-track) sampling. The duty cycle of this so-called optimized
resolution (OR) mode (optimized in terms of a trade-off between spectral and spatial resolution
considering instrument operation safety aspects) could be steadily increased from 30 % in
January 2005 to 100 % from December 2007 on. MIPAS was successfully operated with this
100 full duty cycle in the OR mode until 8 April 2012, when an ENVISAT anomaly occurred
resulting into the loss of communication between ground and satellite and the end of MIPAS
observations (ESA, 2012). Details of the characteristics of the two MIPAS mission phases (FR
and OR modes) in terms of instrument settings and atmospheric sampling are described in
Raspollini et al. (2013).

105 The coarser spectral but finer spatial sampling of MIPAS since 2005 along with the need for
near real time analysis demanded adaptations in the calibration scheme and the processing
codes. This was realized in ESA Level (L) 2 processor version (v) 6 and explained by Raspollini
et al. (2013), which also provides the diagnostics of the products including the error budgets as
estimated by Dudhia et al. (2002). The whole MIPAS data set covering almost 10 years of
observations was re-processed with v6, v7, and v8. In addition, the number of retrieved
110 constituents was extended to ClONO₂, N₂O₅, CFC-11, and CFC-12 in ESA version 6.

ESA version 7 data (released in 2015) also includes the species HCN, HCFC-22, CF₄, COF₂,
and CCl₄. The ESA L1v8/L2v8 diagnostic data set (DDS) version was released in June 2018
followed by the L1v8/L2v8 full mission (FM) data in June 2019. The new v8 data release (ESA,
2021; Dinelli et al., 2021; Raspollini et al., 2022) comprises the additional molecules C₂H₂,
115 C₂H₆, COCl₂, OCS, CH₃Cl, and HDO. For the final ESA reprocessing of MIPAS data,
numerous improvements were implemented in the L2 processor Optimised Retrieval Model
(ORM) version 8.22 (v8) and its auxiliary data including an update of the spectroscopic data
used (Raspollini et al., 2022). All molecules except HDO have been validated by comparison
with observations of the MIPAS balloon instrument.

120 2.2 MIPAS-B data set

The balloon-borne limb-emission sounder MIPAS-B can be regarded as a precursor of the
MIPAS satellite instrument (Friedl-Vallon et al., 2004). Hence, a number of specifications like
spectral resolution and spectral coverage are similar. The unapodized full spectral resolution is
0.0345 cm⁻¹, which is slightly coarser than the FR mode resolution but higher than the OR mode



125 resolution. However, for essential parameters the MIPAS-B performance is superior, in terms
of NESR (Noise Equivalent Spectral Radiance) and line of sight (LOS) stabilization. The LOS
is stabilized using an inertial navigation system supplemented with an additional star reference
system which leads to an after all knowledge of the tangent altitude of better than 50 m at the
1 σ confidence limit (Wetzel et al., 2010). The MIPAS-B NESR is further improved by
130 averaging multiple spectra recorded at the same elevation angle. The general data processing
from interferograms to calibrated spectra including instrument characterization is described in
Friedl-Vallon et al. (2004) and references therein.

MIPAS-B measurements were recorded typically at a 1.5 km vertical tangent altitude grid.
Retrieval calculations of temperature and atmospheric trace species were performed at a 1 km
135 grid with a Gauss-Newton iterative method (Rodgers, 2000) using analytical derivative spectra
calculated by the Karlsruhe Optimized and Precise Radiative transfer Algorithm (KOPRA;
Stiller et al., 2002; Höpfner et al., 2002). To avoid retrieval instabilities due to oversampling of
vertical grid points, a regularization approach according to the method described by Tikhonov
(1963) and Phillips (1962) constraining with respect to the first derivative of the a priori profile
140 was adopted. The resulting vertical resolution is typically between 2 and 5 km for the analysed
atmospheric parameters and is therefore comparable or slightly better than the vertical
resolution of the MIPAS satellite instrument. Table 1 gives an overview on the spectral
windows used for the MIPAS-B target parameter retrievals. Different spectral microwindows
within mostly the same molecular bands were used for the MIPAS-E data analysis (Dinelli et
145 al., 2021). Spectroscopic parameters for the calculation of the infrared emission spectra
originate from the high-resolution transmission (HITRAN) molecular absorption database
(Rothman et al., 2009) and a MIPAS dedicated spectroscopic database (Raspolini et al., 2022).
For heavy molecules like CFC-11, CFC-12, HCFC-22, CCl₄, and CF₄, new and improved
infrared absorption cross sections (Harrison, 2015; Harrison, 2016; Harrison et al., 2017) were
150 used for the calculation of radiative transfer (consistent to the MIPAS-E retrieval).

The MIPAS-B error budget includes random noise as well as covariance effects of the fitted
parameters, temperature errors, pointing inaccuracies, errors of non-simultaneously fitted
interfering species, and spectroscopic data errors (1 σ). For further details on the MIPAS-B data
analysis and error estimation, see Wetzel et al. (2012; 2015) and references therein. An
155 overview of typical errors for the atmospheric parameter retrieval is given in Table 1.



2.3 Validation approach

A number of MIPAS balloon flights have been carried out as part of the validation program of the chemistry instruments aboard ENVISAT. Most of the MIPAS-B data used here, however, were obtained during flights that were done in the framework of various scientific projects.

160 MIPAS-B had a sophisticated pointing system so that the full freedom of a balloon-borne limb emission sounder in terms of observation time, viewing direction and sampling strategy could be used to get the best possible coincidence in time and space with the satellite overpass even during balloon flights that were not primarily dedicated to satellite validation. If compliant with the scientific goal of the mission and the weather conditions, the strategy was to launch the

165 balloon in due time before an ENVISAT overpass and to optimize the azimuthal viewing direction and the vertical sampling at the time of the overpass. Except for two flights, a coincidence in space and time between both sensors could be achieved such that vertical profiles of both instruments can be directly compared. An overview of the MIPAS balloon flights used in this study is given in Table 2.

170 To enhance the statistics of profile comparisons, diabatic 2-day forward and backward trajectories were calculated by the Free University of Berlin using a trajectory model (Naujokat and Grunow, 2003; Grunow, 2009). The trajectories are based on European Centre for Medium-Range Weather Forecasts (ECMWF) 1.25°x1.25° analyses and start at different altitudes at the geolocation of the balloon observation to search for a coincidence with the satellite

175 measurement along the trajectory path within a match radius of 1 h and 500 km. Temperature and volume mixing ratio (VMR) of the satellite match have been interpolated to the trajectory match altitude such that these values can be directly compared to the MIPAS-B data at the trajectory start point altitude. Altitude differences between the trajectory start and match point have to be taken into account in the case of temperature by means of an adiabatic correction.

180 The handling of the diurnal variation of photochemically active species is discussed below.

The primary vertical coordinate of MIPAS-E is pressure whereas for MIPAS-B it is altitude. For all intercomparisons shown in this study, vertical profiles refer to the MIPAS-B pressure-altitude grid. Differences between measured quantities of MIPAS-E and the validation instrument MIPAS-B are expressed in absolute and relative units. The mean difference Δx_{mean}

185 for N profile pairs of compared observations is given as:



$$\Delta x_{mean} = \frac{1}{N} \sum_{n=1}^N (x_{E,n} - x_{B,n}), \quad (1)$$

where x_E and x_B are data values of MIPAS-E and MIPAS-B at one altitude level respectively. The mean relative difference $\Delta x_{mean,rel}$ of a number of profile pairs is calculated by dividing the mean absolute difference by the mean profile value of the reference instrument MIPAS-B:

$$\Delta x_{mean,rel} = \frac{\Delta x_{mean}}{\frac{1}{N} \sum_{n=1}^N x_{B,n}} \cdot 100\% \quad (2)$$

Differences are displayed together with the combined errors σ_{comb} of both instruments, which are defined as:

$$\sigma_{comb} = \sqrt{\sigma_E^2 + \sigma_B^2}, \quad (3)$$

where σ_E and σ_B are the precision, systematic or total errors of MIPAS-E and MIPAS-B, respectively.

Precision errors characterize the reproducibility of a measurement and correspond, in general, to random noise errors. Systematic errors used for the MIPAS-E data analysis have been assessed in corresponding studies (Dudhia et al., 2002; Raspollini et al., 2013; Dinelli et al., 2021). The uncertainty of the calculated mean difference (standard error of the mean, SEM) is given by $\sigma/N^{0.5}$ where σ is the standard deviation (SD). A bias between both instruments is considered significant if the SEM is smaller than the bias itself. The comparison between the VMR difference and the combined systematic error (for statistical comparisons) or total error (for single comparisons) is appropriate to identify unexplained biases in the MIPAS-E measurements when they exceed these combined error limits. Since the vertical resolution of the atmospheric parameter profiles of both instruments is of comparable magnitude, a smoothing by averaging kernels has not been applied to the observed profiles. The method described above was performed for each individual balloon flight comparison. A mean difference (with mean statistical parameters) for all flights was calculated by weighting the mean result of each individual flight equally.

Photochemically reactive gases like NO_2 and N_2O_5 , and, to a lesser extent, ClONO_2 (mainly in the Tropics) undergo a diurnal variation with changing solar zenith angle (SZA). For these gases, a photochemical correction taking into account differences in the SZA between the



215 measurements of both sensors has been applied. The molecule NO_2 exhibits the most pronounced temporal variation. The partitioning of NO , NO_2 , and N_2O_5 within the NO_y family depends strongly on the SZA due to the rapid photolysis of NO_2 and the slower photolysis of N_2O_5 . A 1-dimensional model (Bracher et al., 2005) was constrained with NO_y species measured by MIPAS-B and initialized with the output of a global 2-dimensional model (Sinnhuber et al., 2003) to calculate SZA correction factors for the MIPAS-E data.

220 3 Intercomparison results

In the following subsections we discuss the validation for all quantities delivered operationally by ESA's L1v8/L2v8 FM processor on the basis of collocated MIPAS-B observations. Only MIPAS satellite data that have passed the a posteriori quality check (mainly retrieval convergence and size of maximum error) were used for the intercomparison. The analysis of
225 all compared vertical profiles is regarded as evaluation with the highest statistical evidence. Trajectory matches are based on diabatic 2-day forward and backward trajectories with a collocation criterion of 1 h and 500 km as described in section 2.

Since the balloon flights were performed between 2003 and 2011, they cover almost the full ENVISAT operational period of 2002 to 2012, i.e., both MIPAS-E mission phases (FR and OR
230 modes) with distinctly different instrument settings. A compilation of all vertical profiles of temperature and 20 species retrieved from MIPAS-B spectra is given in Fig. 1. We performed the intercomparison analysis separately not only for different climatological regions but also for the periods 2002-2004 and 2005-2012. The following intercomparison is focused on these two periods when MIPAS-E was operated in the FR and OR mode, respectively. An overview
235 of the most important findings of this intercomparison is listed in Table 3. A comprehensive MIPAS quality readme file including MIPAS-B, ground-based and ACE-FTS (Atmospheric Chemistry Experiment – Fourier Transform Spectrometer) validation results was published by Raspollini et al. (2020).

3.1 Temperature

240 Apart from its relevance as primary atmospheric state parameter, the quality of temperature data is essential in the atmospheric emission limb sounding since temperature profiles generally are retrieved prior to the trace gas retrievals. Hence, temperature errors propagate in subsequent retrievals of trace constituents. Our study shows that above about 11 km the mean differences



between MIPAS-B and MIPAS-E are within ± 2 K and within the combined systematic errors,
245 although the standard deviations exceed the expected precision (see Fig. 2). In the lowermost
stratosphere and around the tropopause, MIPAS-E exhibits a positive bias with respect to the
balloon instrument in the OR mode and the Tropics. Differences between both sensors are
comparable to the findings of a comprehensive temperature validation study by Ridolfi et al.
(2007) that was addressing the FR mode period only using version 4.61 and 4.62 data. However,
250 the large temperature differences between MIPAS-E and MIPAS in the tropical troposphere are
not seen in a comparison to groundbased data (Hubert et al., 2020). A possible reason for this
difference between both MIPAS sensors could be an inaccuracy in the altitude assignment,
which has a particularly strong effect in combination with the strong vertical temperature
gradient in the troposphere.

255 3.2 H₂O

In view of the ongoing debates on long-term trends of water vapour (e.g. Dessler et al., 2014;
Lossow et al., 2018; Khosrawi et al., 2018) we carefully looked at the consistency of the
validation results of the MIPAS FR phase with respect to the MIPAS OR phase. Figure 3
presents the intercomparison results. FR and OR mode comparisons show different vertical
260 shapes of the differences between MIPAS-E and MIPAS-B. In the lowermost stratosphere and
upper troposphere, MIPAS-E significantly overestimates H₂O and exceeds the combined
systematic error bars around 15 km in the OR mode. This general behaviour remains also in the
statistical analysis of all collocations. In the middle and upper stratosphere, a positive bias of
MIPAS-E against MIPAS-B (increasing with altitude in the FR period) of 5-20 % is visible,
265 although the errors stay (except at 37 km) within the predicted error budget. These findings are
in line with the conclusions drawn from a comprehensive validation study of MIPAS-E (version
4.61) phase one (FR mode) observations by Wetzell et al. (2013a). The pronounced deviation
between both MIPAS sensors in the tropical troposphere may possibly be explained by an
inaccuracy in the altitude assignment in combination with the strong vertical H₂O gradient in
270 this altitude region.

3.3 O₃

The monitoring of the expected recovery of the stratospheric ozone layer, and in particular the
Antarctic ozone hole, still remains of great scientific interest (e.g. Dhomse et al., 2019). Hence,
ozone was one of the key species during the ENVISAT mission. Comparisons based on the full



275 statistics over all collocations show an agreement between the satellite and the balloon data
within $\pm 10\%$ above 15 km for this mainly stratospheric species (see Fig. 4). For most of the
stratosphere (17-37 km), the mean relative difference between the data sets is always within
 $\pm 5\%$. Furthermore, differences of the combined FR plus OR mode are within the combined
systematic error. Degradation in the quality of the agreement is observed in the lower
280 stratosphere and upper troposphere, with deviations up to about 20 % in both observation
periods. Generally, the statistical agreement of both data sets is comparable to that reported by
Cortesi et al. (2007) for the FR mode phase (v4.61/v4.62) as deduced from an extensive study
using various kinds of correlative data.

3.4 HNO₃

285 HNO₃ is an important stratospheric nitrogen reservoir species (see e.g. Brasseur and Solomon,
2005). VMR difference profiles of this trace gas are presented in Fig. 5. MIPAS-E tends to
overestimate the HNO₃ abundance when compared to MIPAS-B below about 27 km. This bias
is most prominent in the OR mode data between 19 and 26 km around the altitude of the VMR
maximum of the HNO₃ profile. Biases are typically in the order of 5-20 % in relative units and
290 in line with the numbers reported by Wang et al. (2007) referring to the FR period (v4.61/v4.62).
Standard deviations clearly exceed the expected precision.

3.5 CH₄ and N₂O

These two species are long-lived tracers of similar lifetimes and are therefore correlated to each
other (see e.g. Michelsen et al., 1998). Hence, they are discussed together in this study. Figures
295 6 and 7 present the results for these molecules based on the statistical trajectory analysis of all
collocations available. Both species show a quite similar altitude-dependent behaviour of the
mean difference in absolute and relative quantities while standard deviations exceed the
expected precision. MIPAS-E tends to overestimate the abundance of both species in the
stratosphere below about 35 km by 5-15 % (CH₄) and 10-20 % (N₂O), respectively. A similar
300 positive bias has already been stated in the (FR mode, v4.61) validation study by Payan et al.
(2009). Somewhat larger positive deviations are visible in the Tropics around 30 km.



3.6 NO₂

NO₂ exhibits a strong diurnal variation in the stratosphere and is in photochemical equilibrium with NO and N₂O₅ (see e.g. Brasseur and Solomon, 2005). This needs to be taken into account
305 when comparing NO₂ data sets of different SZA. For our study, a photochemical correction considering differences in the SZA between the measurements of both sensors has been applied as described in more detail in section 2. Figure 8 presents the statistical trajectory match analysis. It indicates a positive bias (up to 20 %, unexplained above 31 km) of MIPAS-E NO₂ in the FR period that is becoming increasingly significant from lower to higher altitudes. This
310 is in line with the findings of the comprehensive NO₂ validation study (FR mode) reported by Wetzel et al. (2007) referring to v4.61 MIPAS data. In the OR period, the positive bias (above 27 km) between both sensors is smaller and amounts to about 10 %.

3.7 Additional v6 products: N₂O₅, ClONO₂, CFC-11, and CFC-12

Starting with processor v6, four additional target species, namely N₂O₅, ClONO₂, CFC-11, and
315 CFC-12, have been operationally processed by ESA. A first validation study of these species was carried out by Wetzel et al. (2013b).

N₂O₅ is a temporary reservoir of reactive nitrogen in the stratosphere and exhibits a prominent diurnal variation with maxima just before sunrise and minima just before sunset (see e.g. Brasseur and Solomon, 2005). The general agreement between MIPAS-E and MIPAS-B is
320 within ±10 % between 24 and 34 km for the mean of all collocations (see Fig. 9). Below 24 km and above 34 km, mean differences exceed at least partly the systematic errors suggesting a careful use of the MIPAS-E N₂O₅ data for scientific studies in these altitude regimes. No significant bias is visible in the OR mode, but a small negative bias is obvious in the FR period. The validation results are in line with the v6 comparison study by Wetzel et al. (2013b).

ClONO₂ is a major reservoir of reactive chlorine in the stratosphere and is involved in heterogeneous chemistry in the context of ozone depletion at high latitudes (e.g. Clarmann and Johansson, 2018, and references therein). It undergoes diurnal variations at higher altitudes during periods of stronger illumination, therefore it had to be photochemically corrected there. Figure 10 presents the intercomparison results for all collocations. In the altitude region where
330 ClONO₂ concentrations are most relevant, both data sets are consistent. Differences are within ±10 % between 17 and 34 km without a clear bias. Only at the upper and lower altitude edge of the comparisons, the mean differences exceed the combined systematic errors. However,



standard deviations clearly exceed the expected precision. The v8 validation results are comparable to the outcome of the study performed by Wetzel et al. (2013b) referring to v6 data.

335 The gases CFC-11 (CCl_3F) and CFC-12 (CCl_2F_2) are rather long-lived chlorofluorocarbons (Ko and Dak Sze, 1982). Results are shown in Figs. 11 and 12, respectively. In the case of CFC-12, mean differences remain within the combined errors and are within $\pm 5\%$ (smaller than in previous versions, not shown in the plots) below 20 km. Above this altitude, a significant positive bias is visible (up to 32 km) and standard deviations exceed the expected precision.

340 However, this bias is less pronounced in the validation studies performed by Engel et al. (2016) and Wetzel et al. (2013b) that were based on observations in comparison to MIPAS v6 data. Deviations for the molecule CFC-11 are somewhat larger with up to $\pm 10\%$ below 20 km. An increasing positive bias is obvious above this altitude level. However, CFC-11 deviations between both MIPAS instruments are smaller compared to the differences shown in the

345 previous validation study by Engel et al. (2016). The improvement in the quality of the CFC-11 v8 data set compared to v6 is also clearly seen in the comparisons to the MIPAS balloon observations (Wetzel et al., 2013b).

3.8 Additional v7 products: HCFC-22, CCl_4 , CF_4 , COF_2 , and HCN

Five more species have been operationally processed by the v7 algorithm. To date, an intercomparison study is only available for vertical VMR profiles of the molecule CCl_4 (Valeri et al., 2017). It should be mentioned that these species are generally more difficult to retrieve than the gases described before. This holds also for the MIPAS-B retrieval, although these gases can be measured with higher accuracy (mainly due to lower spectral noise) compared to MIPAS-E. Hence, some unexplained features (exceeding combined systematic errors) in the

350 VMR difference profiles are expected to occur more frequently when comparing these molecules.

HCFC-22 (CHClF_2) is a longer-lived hydrochlorofluorocarbon. Since HCFC-22 is often used as an alternative to the highly ozone-depleting CFC-11 and CFC-12, its tropospheric concentration is further increasing (e.g. Chirkov et al., 2016). Comparison results are depicted

360 in Fig. 13. In the FR mode period, differences between both instruments remain within $\pm 10\%$ up to 26 km turning into a significant positive bias above this altitude. In the OR observation period, deviations stay within 10 % for altitudes up to 28 km while a significant negative bias



is visible in the MIPAS-E data above this altitude level. Standard deviations exceed the expected precision at higher altitudes (mainly OR phase).

365 The tropospheric mixing ratio of the longer-lived source gas CCl_4 is clearly decreasing since the beginning of the 1990s (Prinn et al., 2000). However, estimated sources and sinks of this molecule are inconsistent with observations of its abundance (Carpenter et al., 2014). A significant negative bias shows up in the MIPAS-E CCl_4 data (full period) above 22 km (see Fig. 14), which is at the brink of the combined systematic error limits. A significant positive bias is visible below 21 km during the OR phase. However, differences stay within $\pm 20\%$ up to about 22 km in both observation periods, which is in line with the deviations reported by Valeri et al. (2017) referring to v7 data.

The fluorocarbon CF_4 has an extremely long atmospheric lifetime of more than 50000 years and its atmospheric concentration is linearly increasing (Carpenter et al., 2014). Comparison results are shown in Fig. 15. A general agreement between both instruments can be stated between 11 and 37 km (within $\pm 10\%$ in both observation periods). In the FR phase, a significant positive bias above 10 km is visible. In contrast, no clear bias is obvious in the OR period where differences stay within $\pm 10\%$ at all altitudes. However, standard deviations exceed the expected precision in the OR phase.

380 The molecule COF_2 is a stratospheric reservoir species for fluorine (Harrison et al., 2014). The general profile shape (as measured by MIPAS-B) is reproduced by MIPAS-E (see Fig. 16). Stratospheric VMR differences stay within $\pm 10\%$ in the FR period and $\pm 20\%$ in the OR period. No unexplained biases (in terms of combined systematic error bars) are evident.

385 HCN is mainly produced by biomass burning and hence considered as an almost unambiguous tracer for biomass burning events (e.g. Li et al., 2003). Differences are within $\pm 20\%$ below 34 km (see Fig. 17). A significant positive bias (more than 20 %) is evident in the MIPAS-E profiles observed in the FR mode period exceeding the combined systematic error limits above 20 km. This pronounced bias is visible in each comparison of the three MIPAS-B flights in the FR phase. No clear bias can be seen in the OR period. The standard deviation between about 390 20 km and 30 km exceeds the estimated precision in the OR phase.

3.9 Additional v8 products: C_2H_2 , C_2H_6 , COCl_2 , OCS , and CH_3Cl

Some more target molecules have been operationally processed by the v8 algorithm. To date, an intercomparison study is only available for vertical VMR profiles of the species COCl_2



(Pettinari et al., 2021). Similar to the additional v7 gases, the emissions of spectral lines of the
395 v8 molecules are also weak compared to the spectral signatures of the standard gases (before
v7). Hence, retrievals of these additional species are challenging.

C₂H₂ is mainly produced by biomass burning and, to a lesser extent, by biofuel burning (e.g.
Singh et al., 1996; Parker et al., 2011; Wiegele et al., 2012). Differences are within $\pm 50\%$ up
to 24 km (see Fig. 18). A significant negative bias (within -50% difference limit) is evident in
400 the FR mode (except for 15-16 km). A significant negative bias below 20 km and above 23 km
can be seen in the OR mode (exceeding combined systematic errors and the -50% difference
limit). Lower stratospheric altitude regions in MIPAS-E retrievals sometimes show negative
VMRs (in Arctic winter). Hence, this species should be carefully used in scientific studies.

C₂H₆ is produced by biomass burning, natural gas losses and fossil fuel production (e.g.
405 Rudolph, 1995; Xiao et al., 2008; Glatthor et al., 2009). Differences are within $\pm 25\%$ up to
19 km (see Fig. 19). While a significant negative bias is obvious in the FR period (exceeding
the -50% limit above 13 km), no bias is seen in the MIPAS-E data below 20 km in the OR
mode, where differences are within a $\pm 20\%$ range. Lower stratospheric altitude regions in
MIPAS-E retrievals sometimes show negative VMRs (in the Arctic). Consequently, C₂H₆
410 profiles should be carefully used in scientific studies.

COCl₂ is produced by chemical industries and OH-initiated oxidation of chlorinated
hydrocarbons in the troposphere (Kindler et al., 1995; Fu et al., 2007; Valeri et al., 2016). Figure
20 shows that differences are within $\pm 20\%$ up to 27 km in both observation periods, such that
the general profile shapes (as measured by MIPAS-B) are reproduced by the satellite
415 instrument. A negative bias is evident in the FR and OR period (except for 22-27 km),
unexplained at high altitudes. Deviations in the Tropics are quite large. The deviations are in
line with the findings of Pettinari et al. (2021) who compared v8 data not only to MIPAS-B but
also to observations from ACE-FTS. Pettinari et al. (2021) found that some of the differences
between MIPAS-E and MIPAS-B can be attributed to the different spectroscopic data used
420 (Toon et al. (2001) for MIPAS-B and Tchana et al. (2015) in the case of MIPAS-E).

OCS is the most prevalent sulphur-containing species which is transported into the stratosphere
where it acts as prerequisite of the stratospheric aerosol layer (Crutzen, 1976; Kremser et al.,
2016; Glatthor et al., 2017). Differences are within $\pm 20\%$ up to 24 km in the FR period and
within $\pm 25\%$ up to 25 km in the OR period (see Fig. 21). A significant positive bias is visible
425 below 22 km and a negative bias above this altitude in the OR period exceeding the $\pm 50\%$ limit



and the combined systematic errors above 24 km. The agreement of the VMR profiles of both sensors is better in the FR period. Here, a significant (positive) bias is only visible between 14 and 18 km. Deviations in the Tropics are quite large.

430 CH₃Cl is the most abundant halocarbon in the atmosphere and originates from natural and anthropogenic sources (see e.g. Yokouchi et al., 2000). Fig. 22 shows that differences stay within ± 20 % between 13 and 22 km (full observation period). However, the comparison reveals a positive bias above 16 km and a negative bias below this altitude in the FR period. A negative bias within -35 % between 19 and 26 km, increasing with altitude, and exceeding the combined systematic errors above 26 km is also visible in the OR period. Large deviations between both
435 instruments occur at midlatitudes and in the Tropics.

4 Conclusions

Vertical profiles of MIPAS balloon flights between 2002 and 2011 covering virtually the whole lifetime of MIPAS on ENVISAT have been used for an intercomparison study of all operational
440 parameters delivered by ESA (except HDO), namely temperature and 20 species as listed in Table 1. The main findings of this intercomparison study are summarized in Table 3. The difference between retrieved temperature profiles of both MIPAS instruments generally stays within ± 2 K in the stratosphere. The MIPAS satellite observations of a large number of gases like H₂O, O₃, HNO₃, CH₄, N₂O, NO₂, N₂O₅, ClONO₂, CFC-11, CFC-12, HCFC-22, CCl₄, CF₄,
445 COF₂, and HCN show an overall good agreement of 5 % to 20 % with the MIPAS balloon measurements in the lower stratosphere.

The intercomparison of the new MIPAS v8 products C₂H₂, C₂H₆, COCl₂, OCS, and CH₃Cl exhibits a somewhat reduced agreement with the MIPAS-B observations compared to the above-mentioned species. However, COCl₂, OCS, and CH₃Cl achieve a 20-percent agreement
450 at least in the extratropical upper troposphere and lower stratosphere.

Overall it can be stated that the v8 operational MIPAS data can be recommended for scientific use. However, data users are strongly advised to consider the findings presented in this study in the respective sections and in Table 3 when using the MIPAS data. A comprehensive MIPAS quality readme file including MIPAS-B, ground-based and ACE-FTS validation results was
455 published by Raspollini et al. (2020) and is recommended for data users who want to get more detailed information on the quality of MIPAS data.



Data availability. MIPAS operational satellite data are available at the European Space Agency mission web page (<https://doi.org/10.5270/EN1-c8hgqx4>, last access: 12 July 2022). MIPAS
460 balloon data are available upon request (<https://www.imk-asf.kit.edu/ffb.php>, last access: 12 July 2022).

Author contributions. GW wrote the paper and performed the bulk of the MIPAS balloon data analysis, with input from all co-authors. AK performed the MIPAS-B Level 1 data processing.
465 MH provided the retrieval software. FFV and GM operated the balloon instrument during all campaigns. HO directed the research and flight planning. MS used a 1-dimensional model for photochemical corrections. JA performed trajectory match calculations. PR had a leading role in evaluating and improving the MIPAS ESA data. AD was the head of the MIPAS Quality Working Group and coordinated the validation activities. All authors commented on and
470 improved the manuscript.

Competing interests. The authors declare that they have no conflict of interest.

Special issue statement. This article is part of the special issue “MIPAS ESA Level 2 version 8
475 products: algorithms, product features and validation”. It is not associated with a conference.

Acknowledgements. Financial support by the DLR (Project 50EE0020) and ESA for the MIPAS balloon flights is gratefully acknowledged. We thank the Centre National d'Etudes Spatiales (CNES) balloon launching team and the Swedish Space Corporation (SSC) Esrange team for
480 excellent balloon operations. An acknowledgement goes to the work performed by the Quality Working Group established by ESA for verification and monitoring of MIPAS products. A corresponding report on the validation activities was published by ESA (Wetzel et al., 2020). We acknowledge support by Deutsche Forschungsgemeinschaft and the Open Access Publishing Fund of Karlsruhe Institute of Technology.

485



Table 1. Overview of MIPAS-B spectral windows used for the analysis of atmospheric target parameters together with typical precision errors and total errors.

Target parameter	Spectral range (cm ⁻¹)	Precision error	Total error
Temperature	801.1 – 813.2	0.2 – 0.3 K	0.5 – 1.0 K
	941.3 – 956.7		
H ₂ O	808.0 – 825.3	1 – 2 %	8 – 11 %
	1210.2 – 1244.5		
	1585.0 – 1615.0		
O ₃	763.5 – 824.4	0.1 – 1 %	8 – 10 %
	964.9 – 969.0		
	1140.1 – 1195.6		
HNO ₃	864.0 – 874.0	0.2 – 2 %	8 – 9 %
CH ₄ & N ₂ O	1161.9 – 1229.8	1 – 3 %	6 – 10 %
NO ₂	1585.0 – 1615.0	1 – 3 %	10 – 12 %
N ₂ O ₅	1220.0 – 1270.0	0.4 – 2 %	5 – 7 %
ClONO ₂	779.7 – 780.7	2 – 3 %	5 – 6 %
CFC-11	840.0 – 860.0	2 – 3 %	5 – 6 %
CFC-12	918.0 – 924.0	2 – 3 %	5 – 6 %
HCFC-22	828.0 – 830.0	3 – 6 %	9 – 12 %
CCl ₄	786.0 – 806.0	5 – 10 %	11 – 15 %
CF ₄	1274.3 – 1288.0	2 – 6 %	6 – 11 %
COF ₂	750.0 – 776.0	1 – 3 %	10 – 12 %
HCN	750.0 – 776.0	4 – 8 %	9 – 12 %
C ₂ H ₂	750.2 – 790.1	5 – 10 %	7 – 12 %
C ₂ H ₆	811.5 – 835.8	8 – 12 %	12 – 15 %
COCl ₂	838.3 – 860.0	2 – 5 %	20 – 22 %
OCS	842.4 – 876.0	15 – 20 %	18 – 25 %
CH ₃ Cl	742.5 – 755.0	5 – 15 %	12 – 20 %



495 **Table 2.** Overview of MIPAS balloon flights used for intercomparison with MIPAS-E. Distances and times between closest trace gas profile pairs observed by MIPAS-E and the validation instrument refer to an altitude of 20 km (Kiruna) and 30 km (Aire sur l'Adour and Teresina). In addition, 2-day forward/backward trajectories were calculated for each balloon flight to search for further matches with the satellite sensor.

Location	Date	Distance (km)	Time difference (min)
Kiruna, 68 °N	20 Mar 2003	16 / 546	14 / 15
	03 Jul 2003	Trajectories only	
	11 Mar 2009	187 / 248	5 / 6
	24 Jan 2010	109 / 302	5 / 6
	31 Mar 2011	Trajectories only	
Aire sur l'Adour, 44 °N	24 Sep 2002	21 / 588 / 410 / 146	12 / 13 / 15 / 16
Teresina, 5 °S	14 Jun 2005	109 / 497 / 184 / 338	228 / 229 / 268 / 269
	06 Jun 2008	224 / 284 / 600 / 194	157 / 158 / 169 / 170

500

505

510



515

Table 3. Summary of MIPAS-E validation results (trajectory comparison to eight MIPAS-B flights). Mentioned atmospheric parameter differences refer to MIPAS-E minus the balloon instrument.

Parameter	Comments (L1v8/L2v8 FM)
Temp.	Differences within ± 2 K between 12 and 39 km.
H₂O	Positive bias (5-20 %) between 11 and 39 km within combined systematic errors (except OR mode around 15 km).
O₃	Differences within ± 10 % for all altitudes above 15 km.
HNO₃	Significant positive bias (5-20 %) below 27 km (most pronounced between 19 and 26 km in the OR mode).
CH₄ & N₂O	Positive bias for CH ₄ (5-15 %) and N ₂ O (10-20 %) below 35 km, especially pronounced for N ₂ O in the lowermost stratosphere around 15 km. Somewhat larger positive deviations also in the Tropics around 30 km.
NO₂	Positive bias of up to 20 % in FR mode (unexplained above 31 km), smaller positive bias (~ 10 %) in OR mode (above 27 km).
N₂O₅	Differences within ± 10 % between 24 and 34 km (no significant bias in OR mode, small negative bias in FR period).
ClONO₂	Differences within ± 10 % between 17 and 34 km (no significant bias).
CFC-11	Differences within 10 % below 20 km. Positive bias (increasing with altitude) above this altitude level.
CFC-12	Differences within ± 5 % for altitudes below 20 km. Significant positive bias above this altitude level up to 32 km.
HCFC-22	Differences within ± 10 % up to 26 km (FR mode) and 28 km (OR mode). Positive differences up to 20 % above 26 km (FR mode) and significant negative bias above 28 km (OR mode).
CCl₄	Differences within ± 20 % up to about 22 km in both observation periods. Increasing negative bias above 22 km (full period).
CF₄	Differences within ± 10 % between 11 and 37 km (both periods). Significant positive bias above 10 km in FR period. No clear bias in OR period.
COF₂	Differences within ± 10 % for FR period and within ± 20 % in OR period in the stratosphere; no unexplained biases.
HCN	Differences within ± 20 % below 34 km. Stratospheric positive bias in FR mode, exceeding combined systematic errors above 20 km (difference > 20 %). No clear bias in OR period.
C₂H₂	Differences within ± 50 % up to 24 km. Negative bias (within 50 %) in FR mode (except 15-16 km), significant negative bias below 20 km and above 23 km in OR mode (exceeding combined systematic errors and the -50 % difference limit). Lower stratospheric altitude regions in MIPAS-E retrievals sometimes show negative VMRs (in Arctic winter).
C₂H₆	Differences within ± 25 % up to 19 km. Significant negative bias in FR mode (exceeding -50 % limit above 13 km), no bias in OR mode below 20 km (differences within ± 20 %). Lower stratospheric altitude regions in MIPAS-E retrievals sometimes show negative VMRs (in the Arctic).
COCl₂	Differences within ± 20 % up to 27 km in both periods. Negative bias in FR and OR period (except 22-27 km), unexplained at high altitudes; quite large deviations in the Tropics. Parts of differences can be attributed to new spectroscopic data (MIPAS-E retrieval).
OCS	Differences within ± 20 % up to 24 km in FR period. Significant positive bias between 14 and 18 km; difference within ~ 25 % up to 25 km (OR mode). Significant positive bias < 22 km and negative bias > 22 km (OR mode) exceeding ± 50 % limit and combined systematic errors above 24 km; quite large deviations in the Tropics.
CH₃Cl	Differences within ± 20 % between 13 and 22 km. Positive bias above 16 km (negative bias below) in FR period. Negative bias within -35 % between 19 and 26 km, increasing with altitude, and exceeding the combined systematic errors above 26 km (OR period). Large deviations at midlatitudes and in the Tropics.

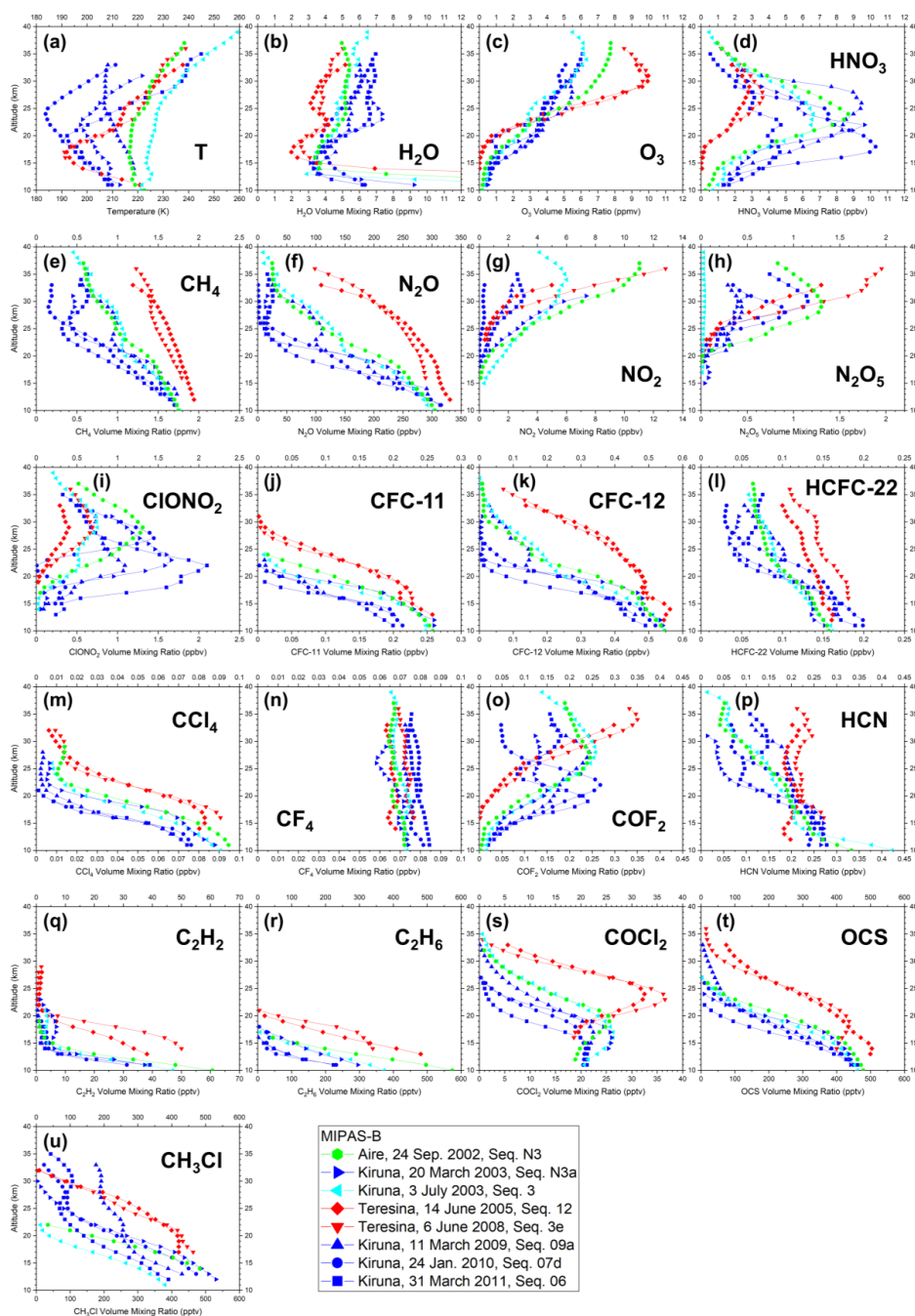


Figure 1. Retrieved vertical profiles of temperature (a) and species (b-u) of Arctic winter (blue), Arctic summer (cyan), midlatitude (green) and tropical (red) MIPAS-B flights as listed in Table 2.

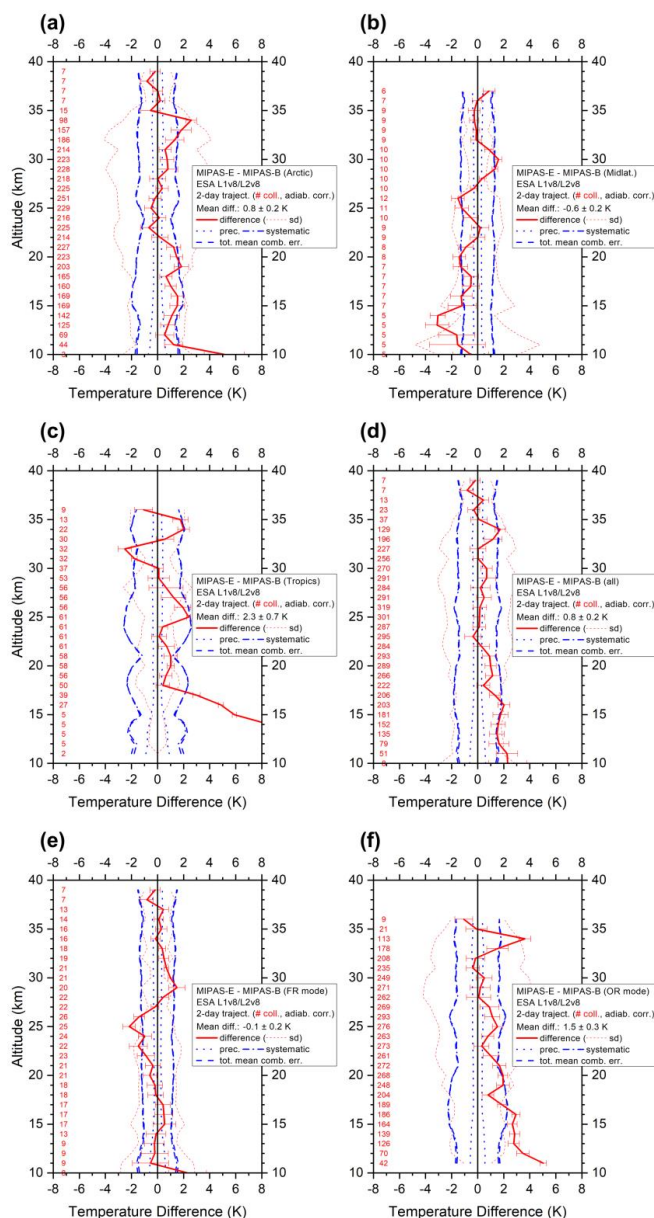


Figure 2. Mean temperature difference (red solid line) of all trajectory match collocations (red numbers) between MIPAS-E and MIPAS-B including standard deviation (red dotted lines) and standard error of the mean (plotted as error bars). Precision (blue dotted lines), systematic (blue dash-dotted lines), and total (blue dashed lines) mean combined errors are shown, too. Arctic (a), midlatitude (b), Tropics (c), all FR plus OR (d), FR mode (e), and OR mode (f) collocations. For details, see text.

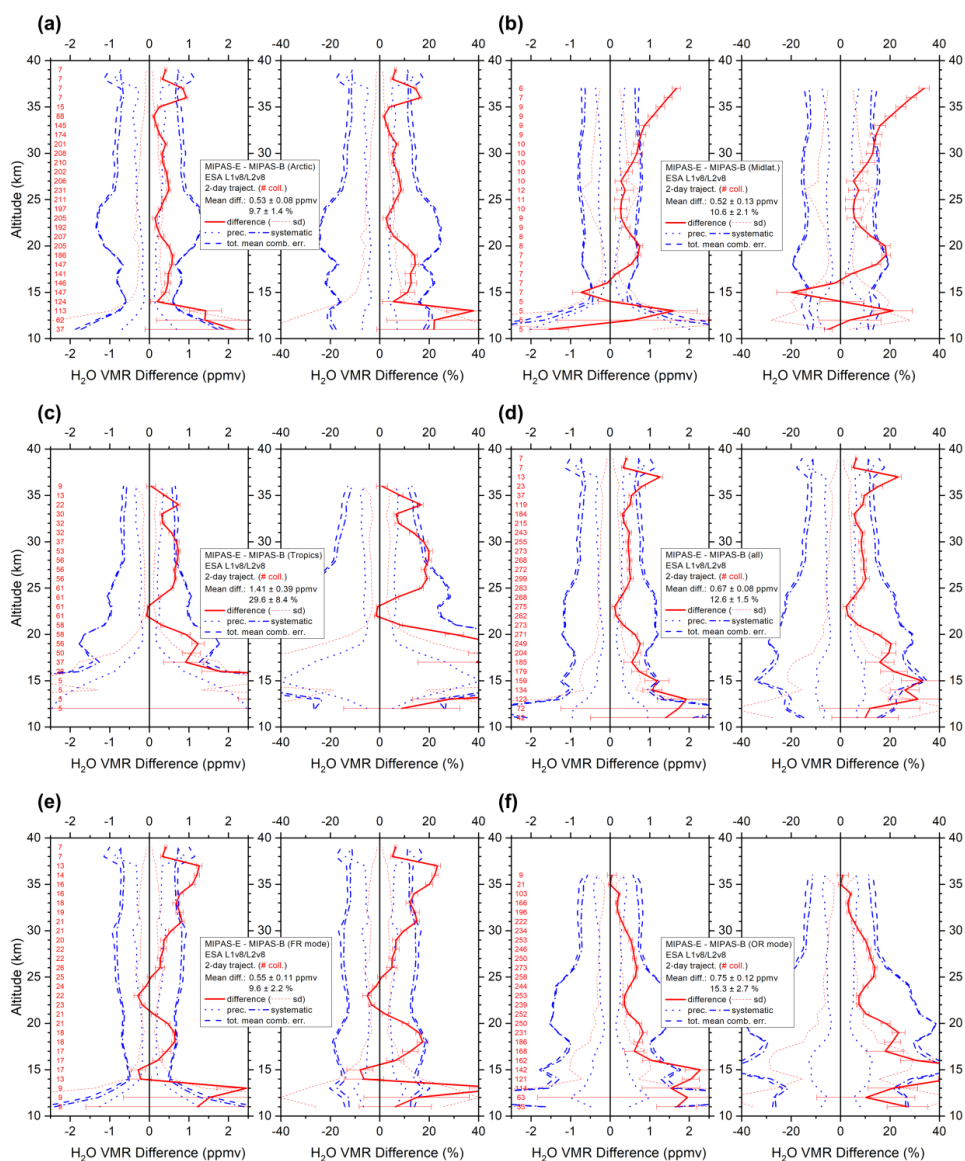


Figure 3. Mean absolute and relative H₂O VMR difference of all trajectory match collocations (red numbers) between MIPAS-E and MIPAS-B (red solid line) including standard deviation (red dotted lines) and standard error of the mean (plotted as error bars). Precision (blue dotted lines), systematic (blue dash-dotted lines), and total (blue dashed lines) mean combined errors are shown, too. Arctic (a), midlatitude (b), Tropics (c), all FR plus OR (d), FR mode (e), and OR mode (f) collocations. For details, see text.

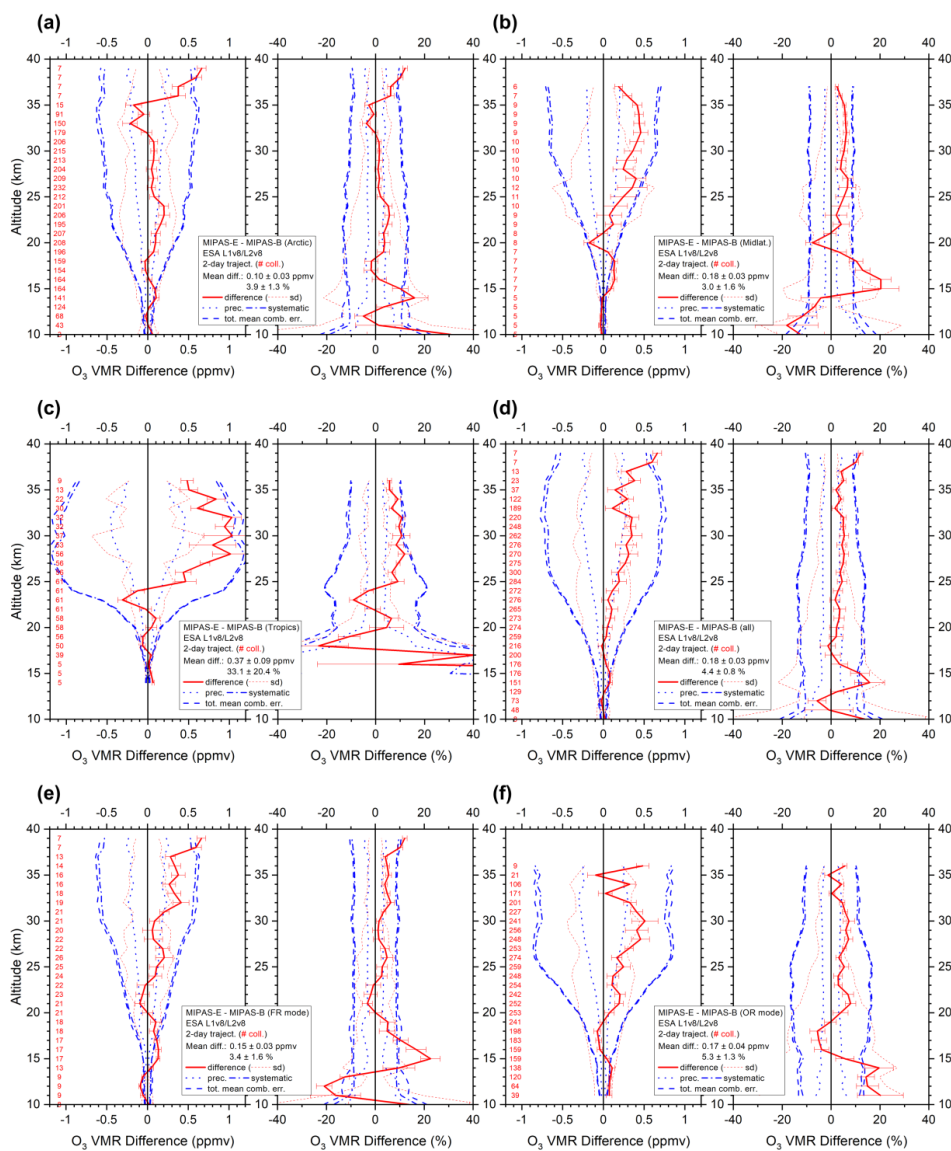


Figure 4. Same as Fig. 3 but for O₃.

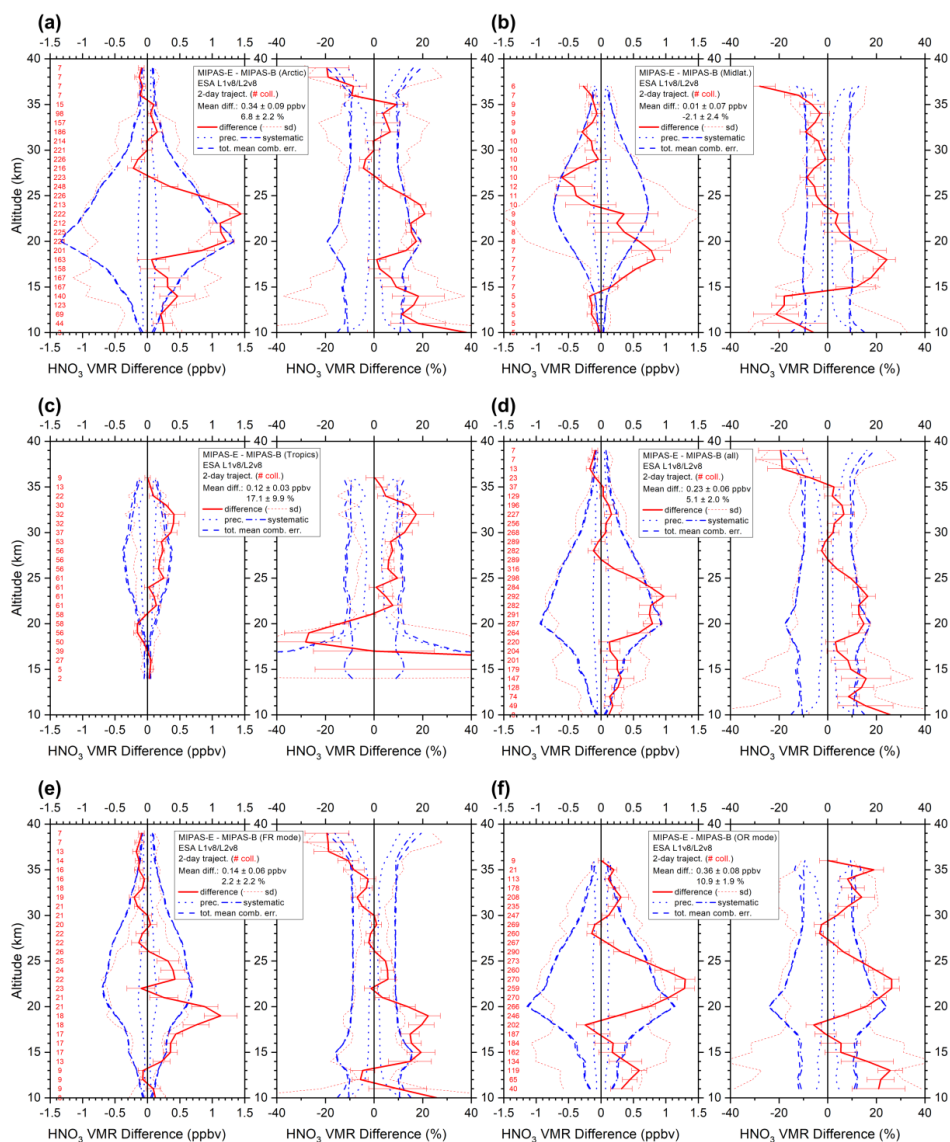


Figure 5. Same as Fig. 3 but for HNO₃.

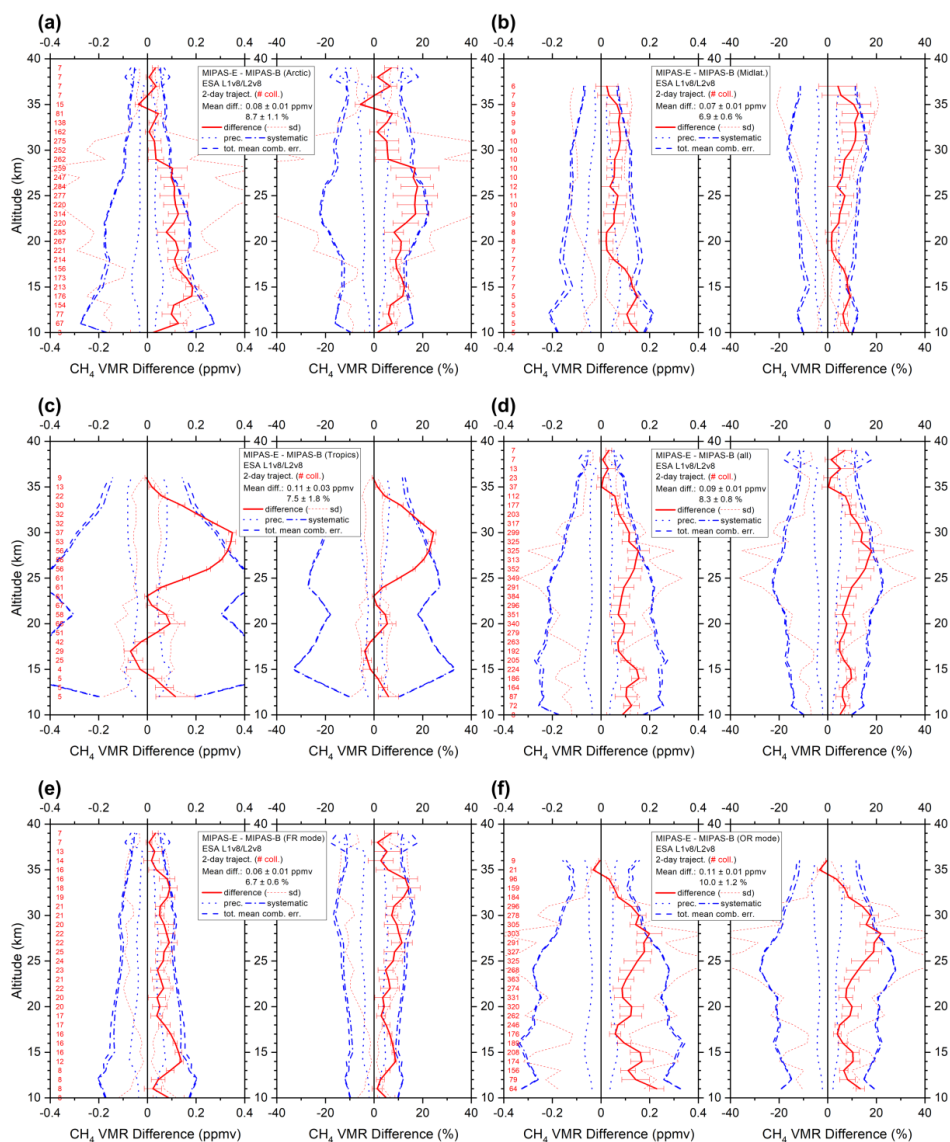


Figure 6. Same as Fig. 3 but for CH₄.

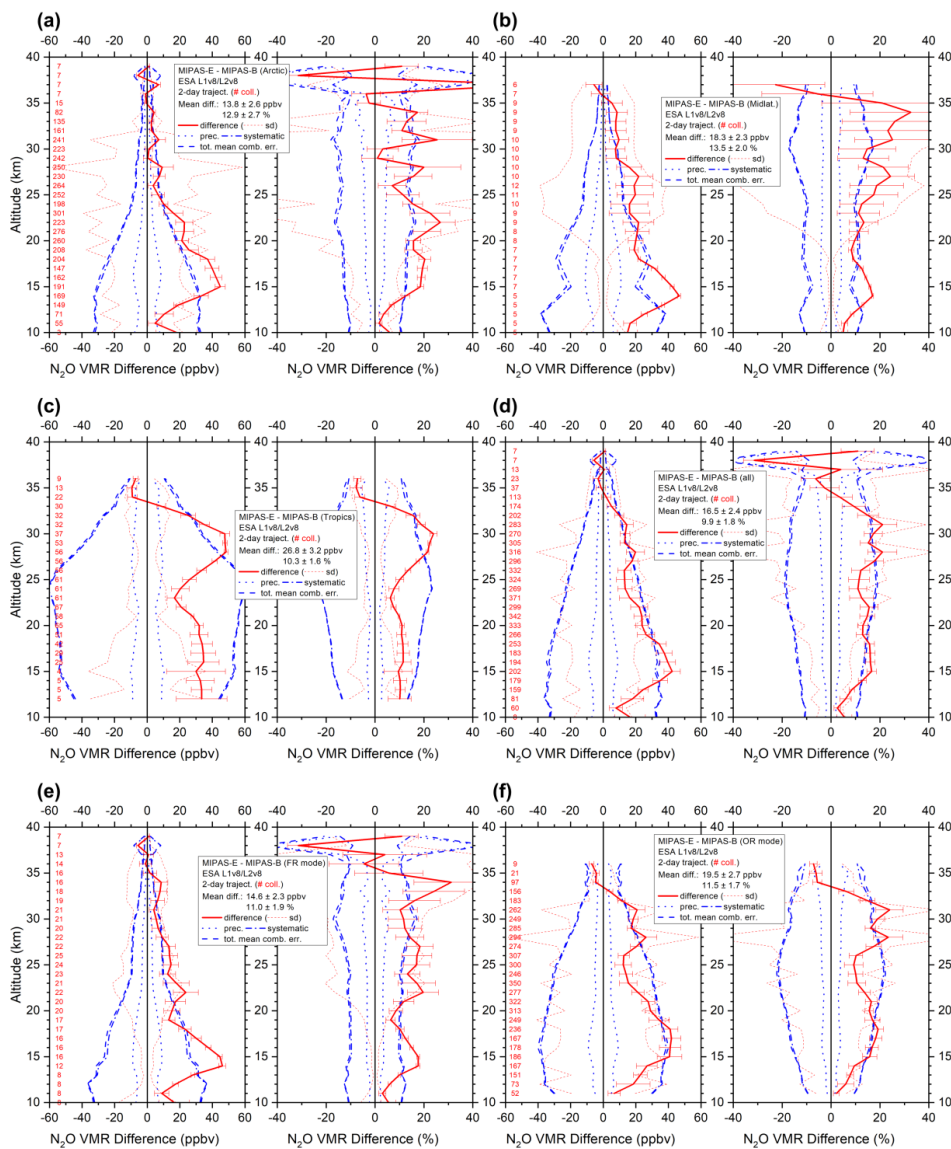


Figure 7. Same as Fig. 3 but for N₂O.

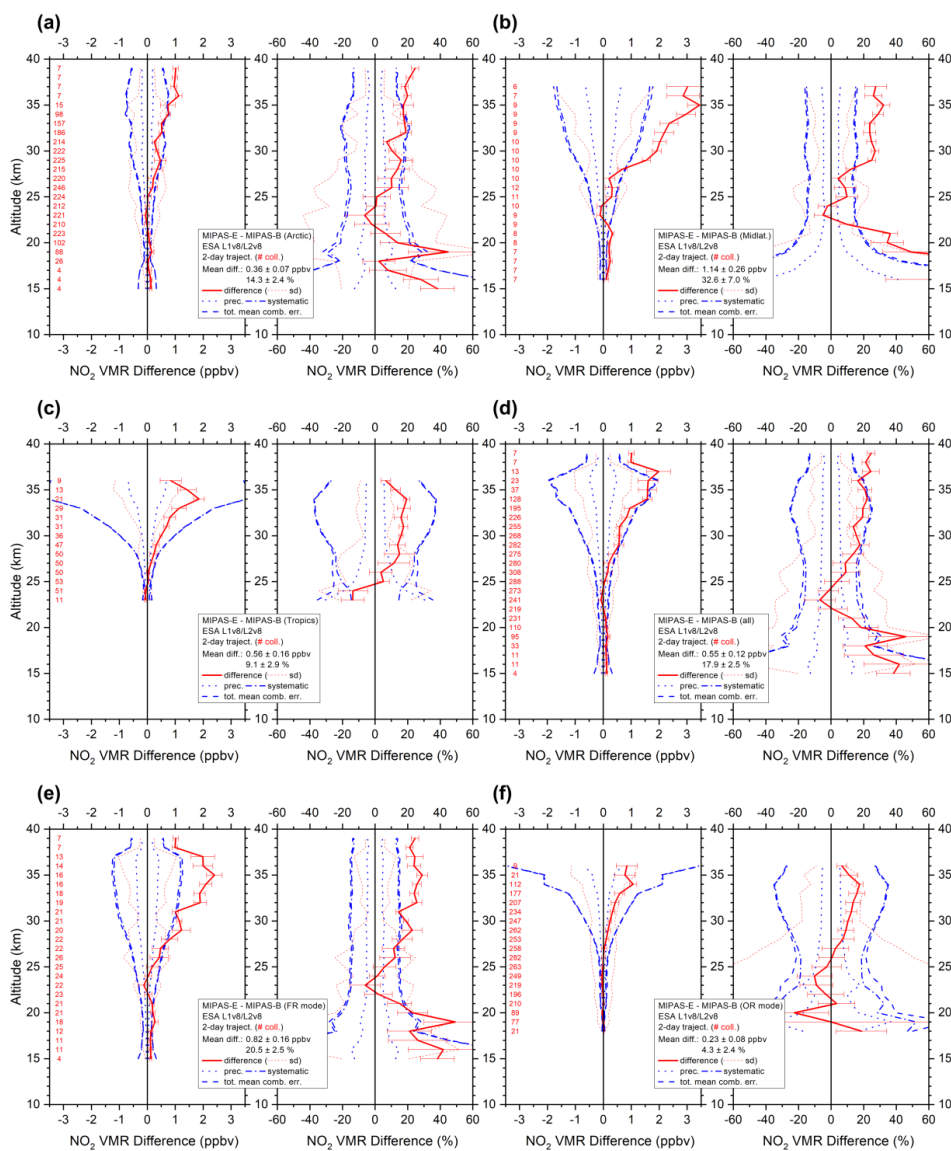


Figure 8. Same as Fig. 3 but for NO₂.

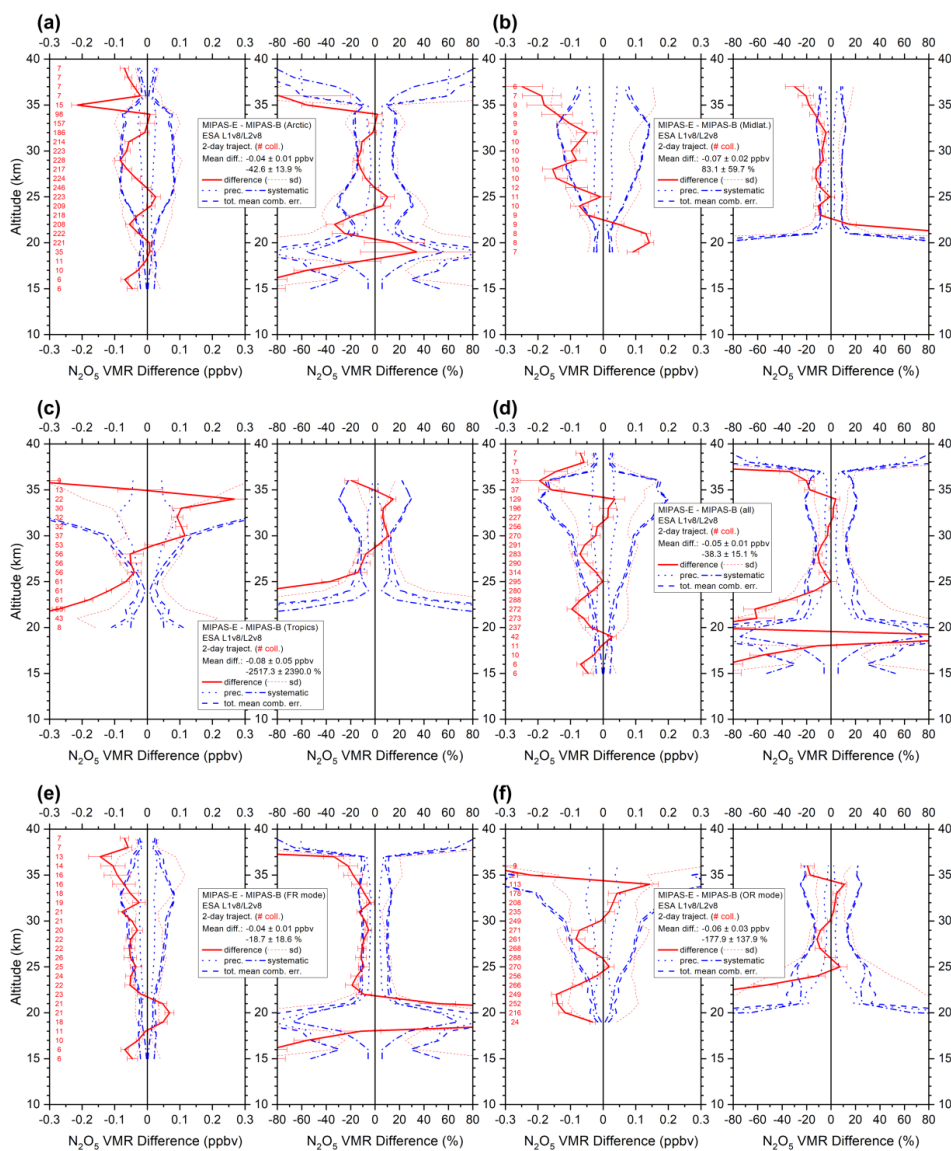


Figure 9. Same as Fig. 3 but for N_2O_5 .

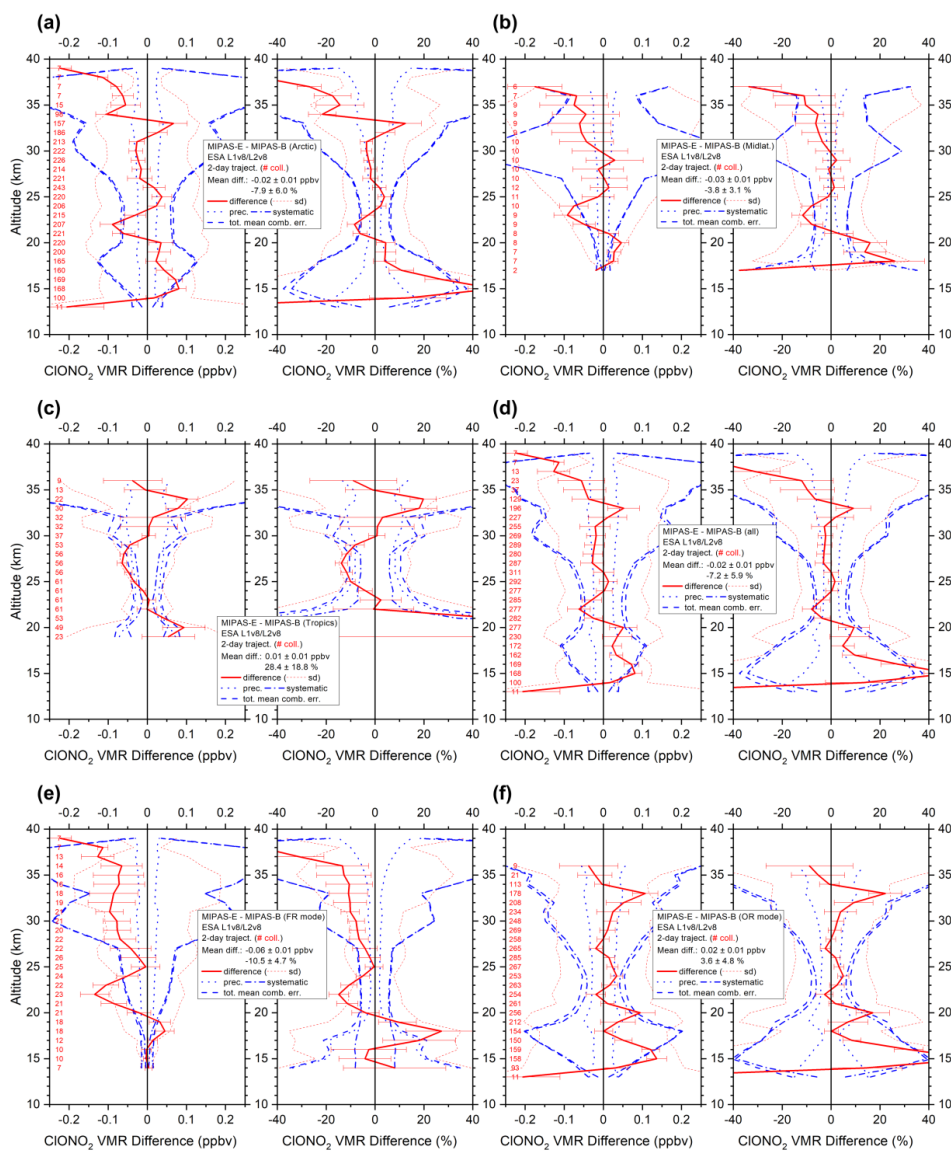


Figure 10. Same as Fig. 3 but for CIONO₂.

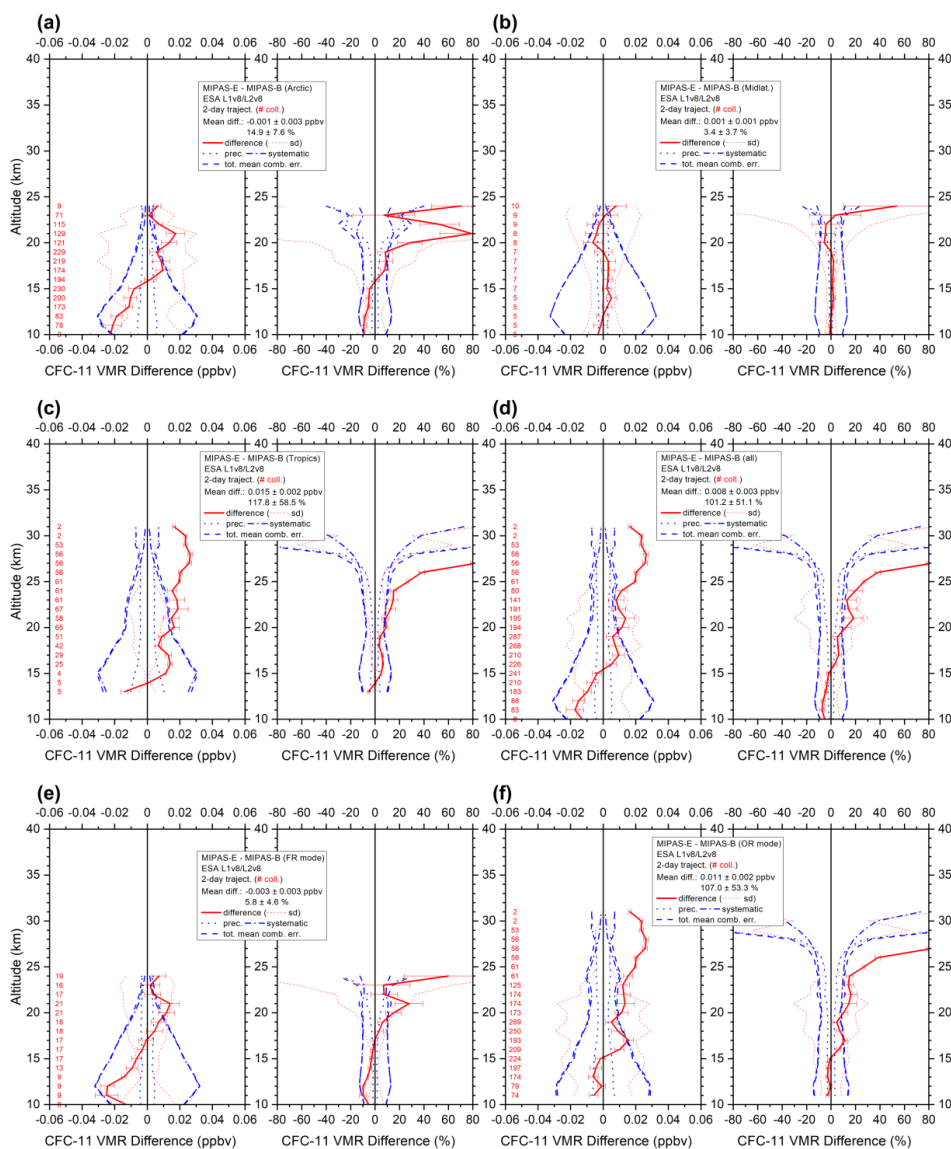


Figure 11. Same as Fig. 3 but for CFC-11.

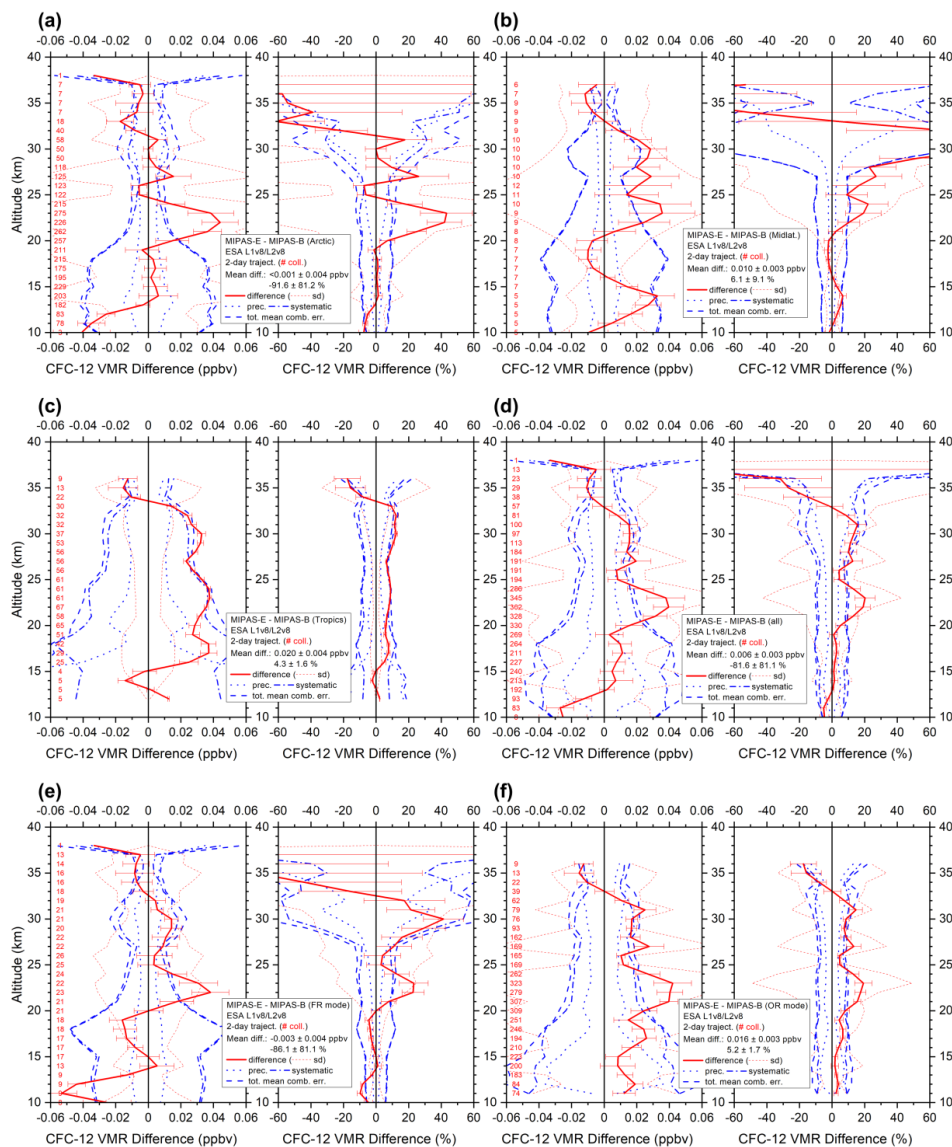


Figure 12. Same as Fig. 3 but for CFC-12.

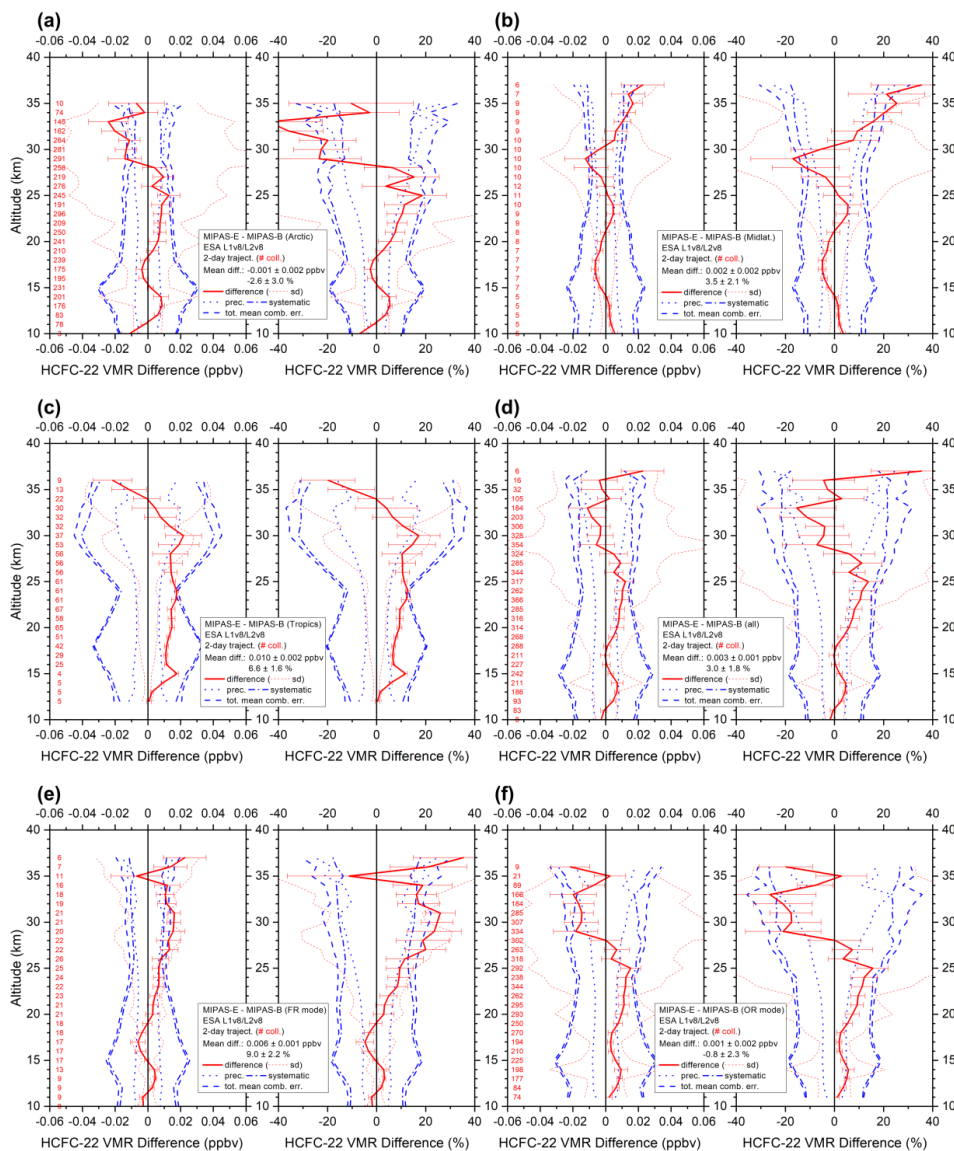


Figure 13. Same as Fig. 3 but for HCFC-22.

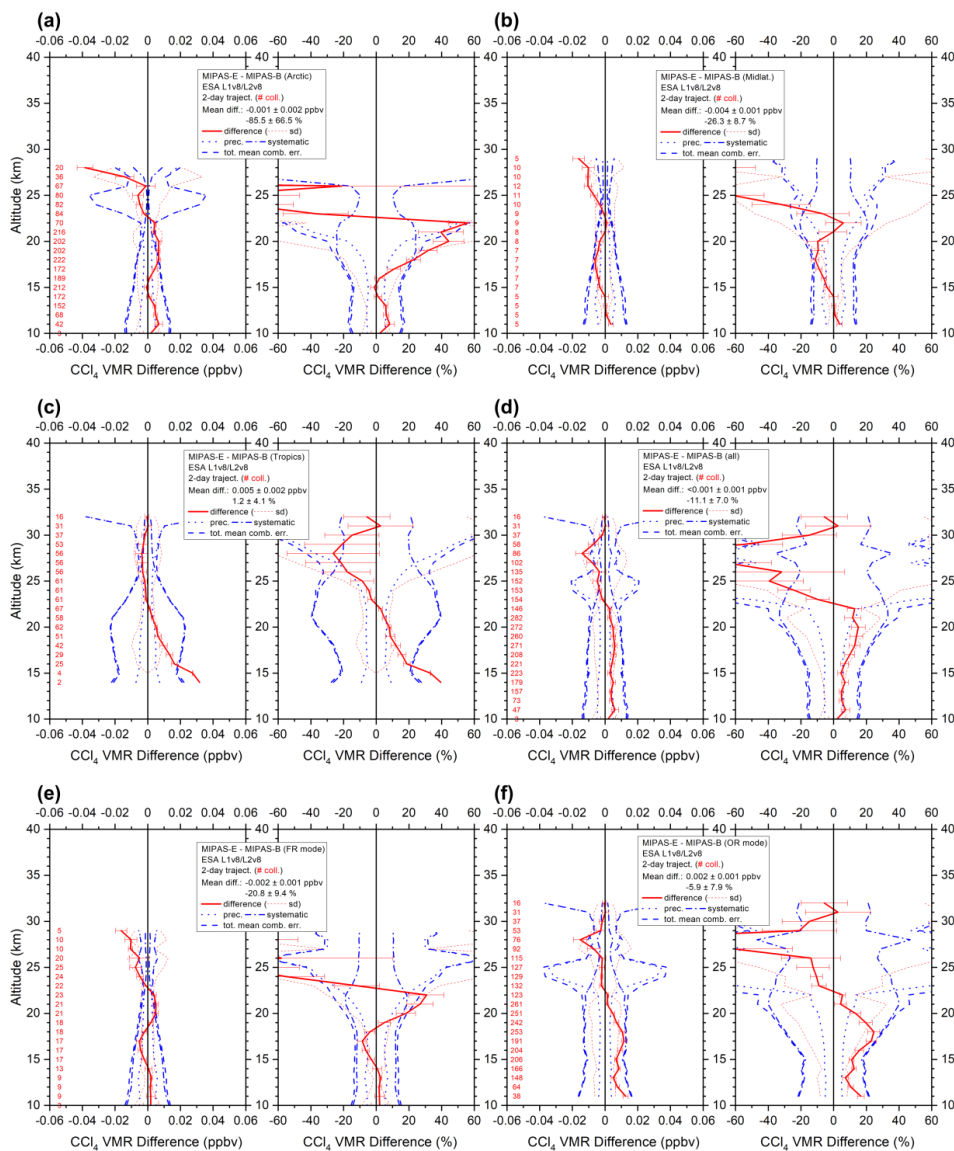


Figure 14. Same as Fig. 3 but for CCl_4 .

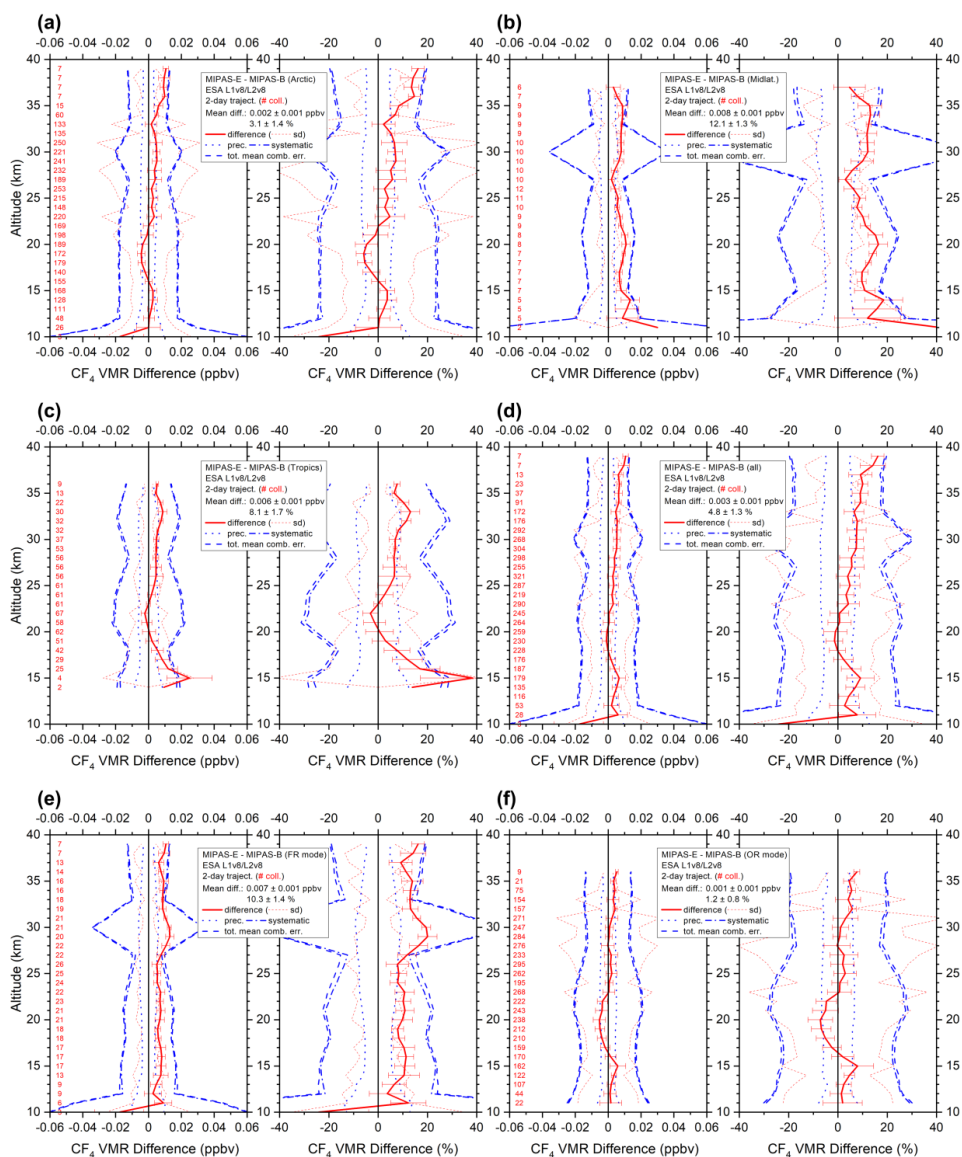


Figure 15. Same as Fig. 3 but for CF₄.

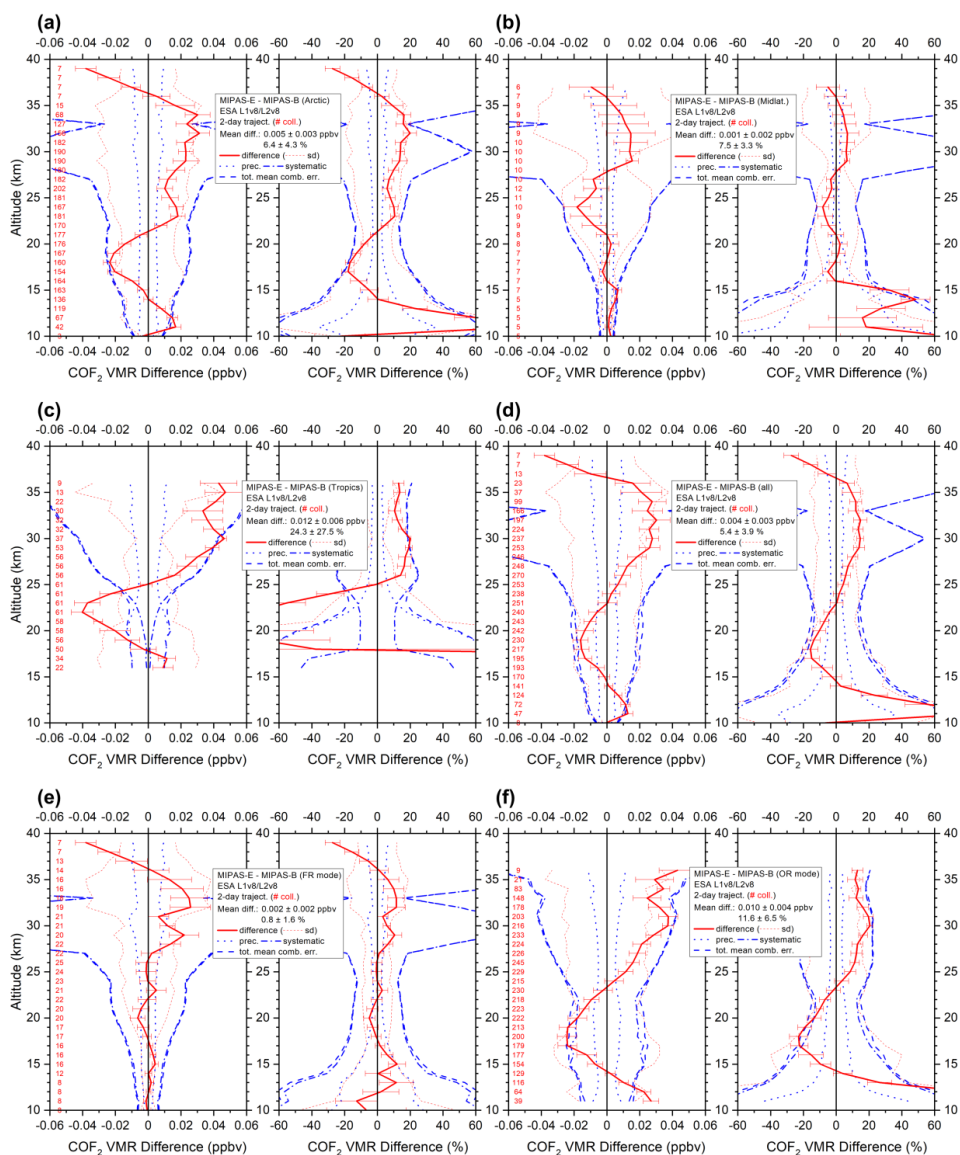


Figure 16. Same as Fig. 3 but for CO₂.

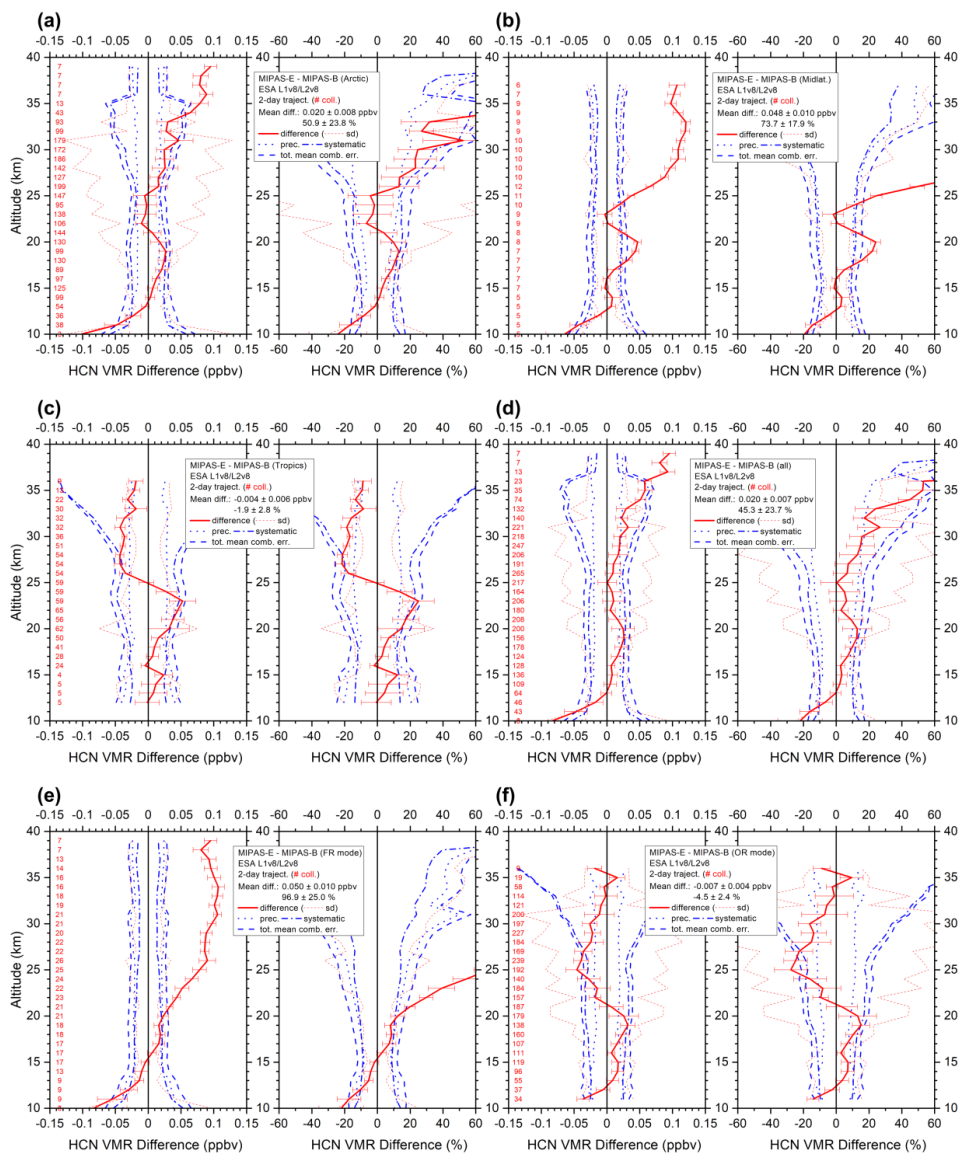


Figure 17. Same as Fig. 3 but for HCN.

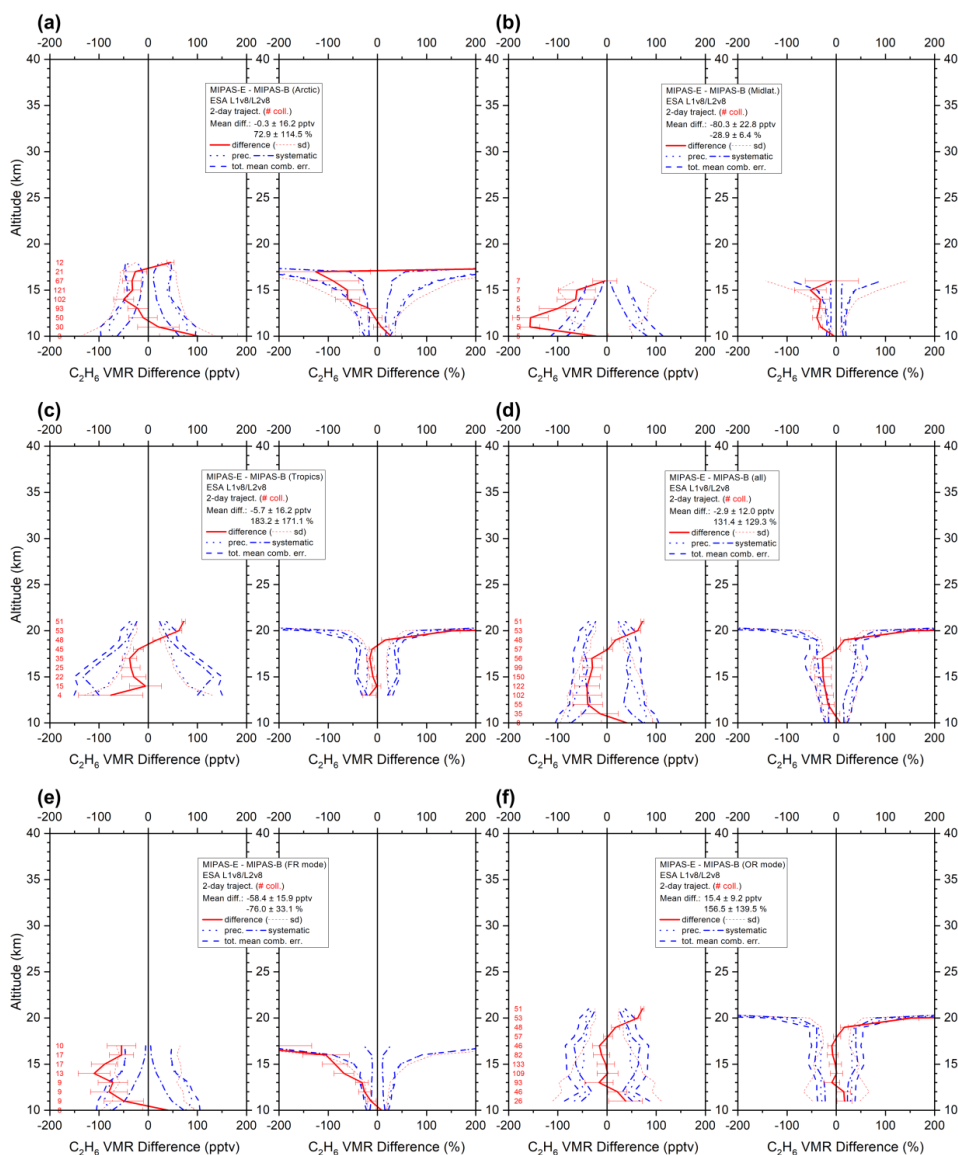


Figure 19. Same as Fig. 3 but for C_2H_6 .

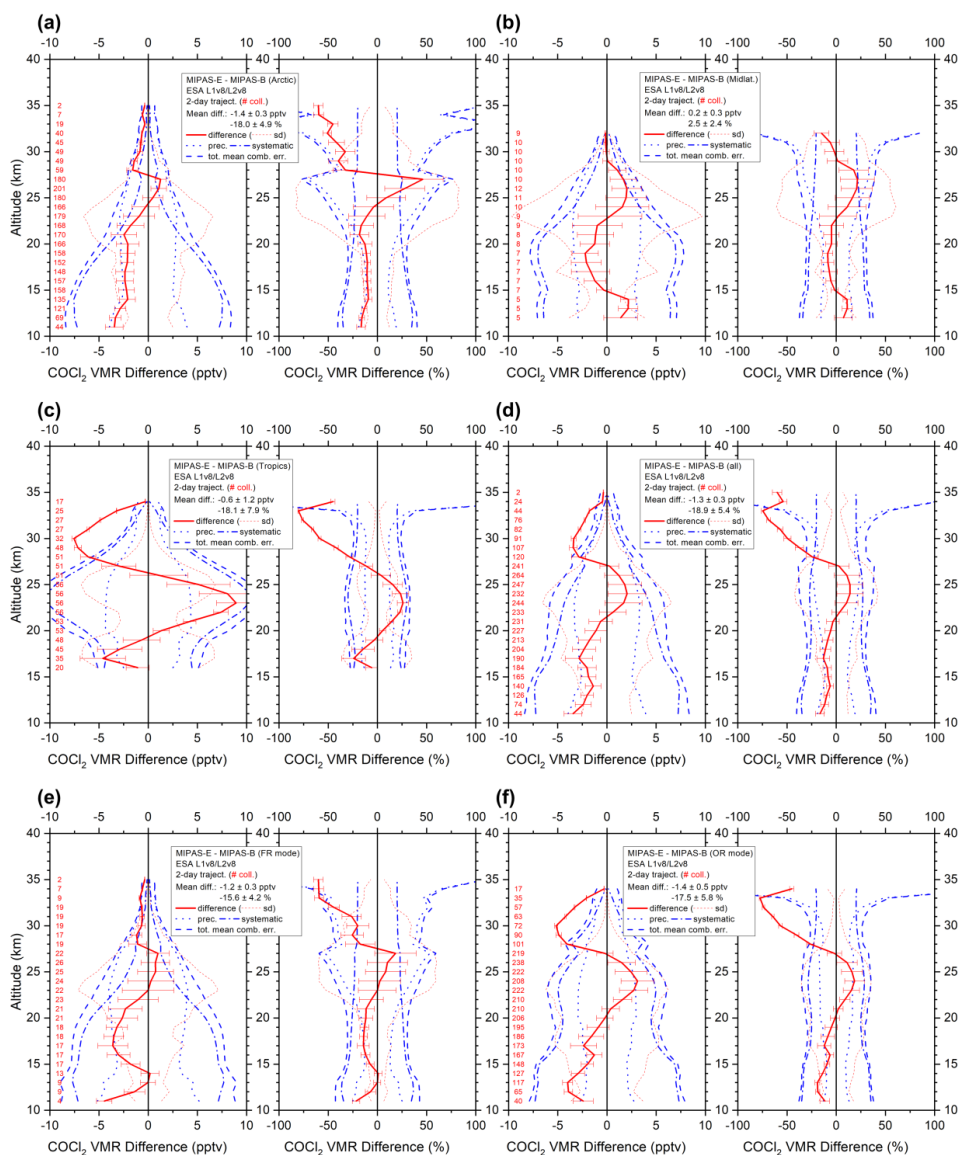


Figure 20. Same as Fig. 3 but for COCl₂.

535

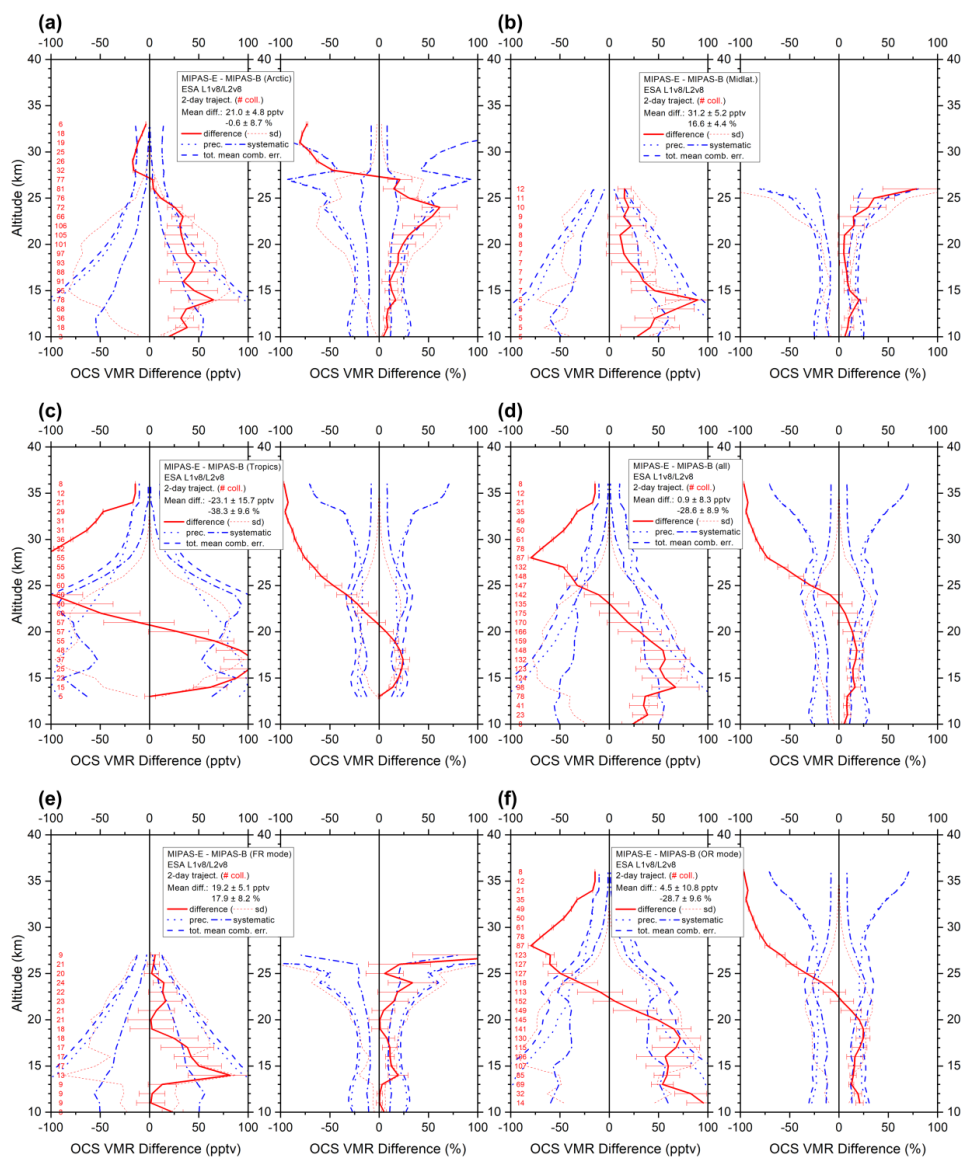


Figure 21. Same as Fig. 3 but for OCS.

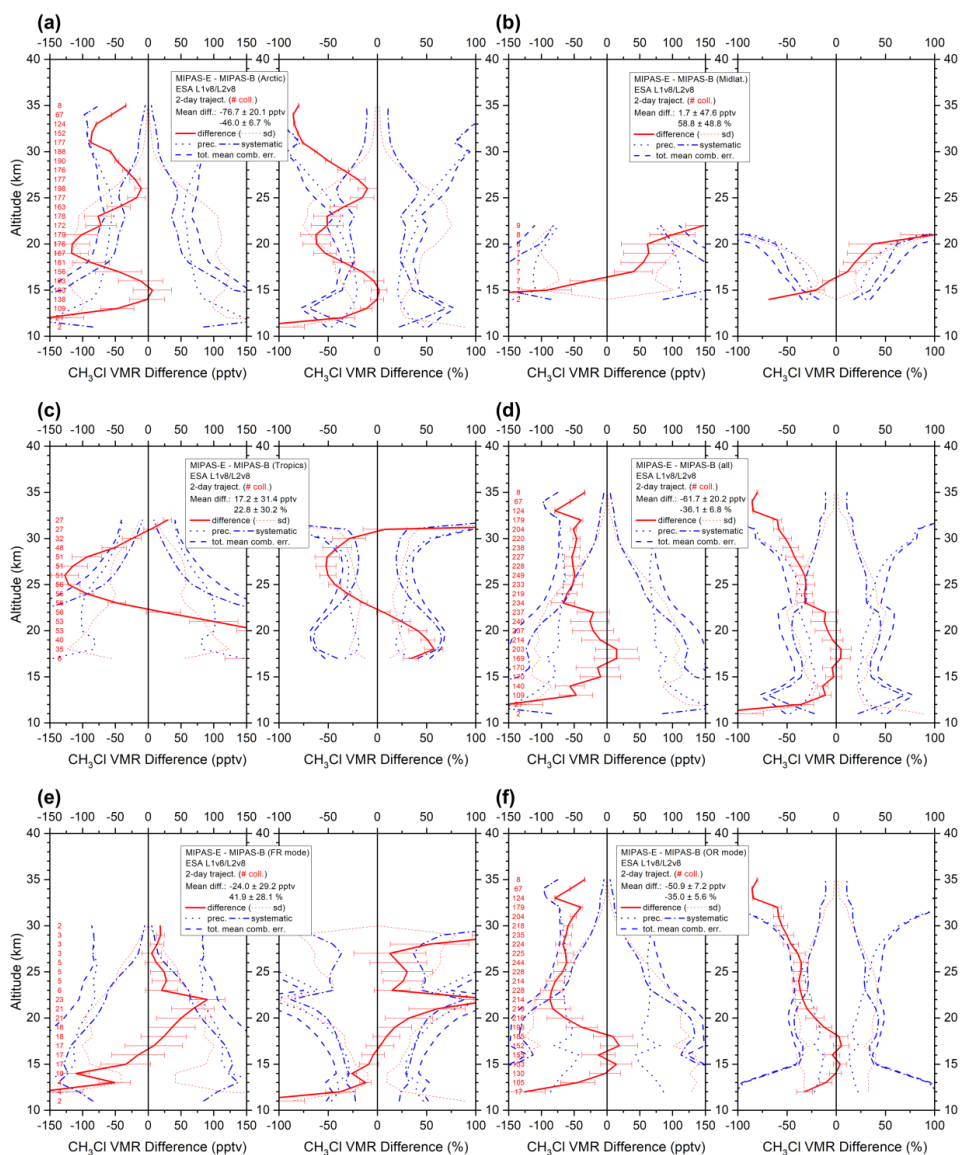


Figure 22. Same as Fig. 3 but for CH₃Cl.



540 **5 References**

- Bertaux, J. L., Mégie, G., Widemann, T., Chassefière, E., Pellinen, R., Kyrola, E., Korpela, S., and Simon, P.: Monitoring of ozone trend by stellar occultations: the GOMOS instrument, *Advances in Space Research*, 11, 237–242, [https://doi.org/10.1016/0273-1177\(91\)90426-K](https://doi.org/10.1016/0273-1177(91)90426-K), 1991.
- 545 Bovensmann, H., Burrows, J. P., Buchwitz, M., Frerick, J., Noël, S., Rozanov, V. V., Chance, K. V., and Goede, A. P. H.: SCIAMACHY: Mission Objectives and Measurement Modes, *J. Atmos. Sci.*, 56, 127–150, [https://doi.org/10.1175/1520-0469\(1999\)056<0127:SMOAMM>2.0.CO;2](https://doi.org/10.1175/1520-0469(1999)056<0127:SMOAMM>2.0.CO;2), 1999.
- Bracher, A., Sinnhuber, M., Rozanov, A., and Burrows, J. P.: Using a photochemical model
550 for the validation of NO₂ satellite measurements at different solar zenith angles, *Atmos. Chem. Phys.*, 5, 393–408, <https://doi.org/10.5194/acp-5-393-2005>, 2005.
- Brasseur, G. P. and Solomon, S.: *Aeronomy of the Middle Atmosphere: Chemistry and Physics of the Stratosphere and Mesosphere*, Third revised and enlarged edition, Atmospheric and Oceanographic Sciences Library, 32, Springer, Dordrecht, 2005.
- 555 Carpenter, L. J., Reimann, S., Burkholder, J. B., Clerbaux, C., Hall, B. D., Hossaini, R., Laube, J. C., and Yvon-Lewis, S. A.: Chapter 1: Update on Ozone-Depleting Substances (ODSs) and Other Gases of Interest to the Montreal Protocol, in: *Scientific Assessment of Ozone Depletion*, edited by: Ennis Christine A., World Meteorological Organization (WMO), 21–125, 2014.
- 560 Chirkov, M., Stiller, G. P., Laeng, A., Kellmann, S., von Clarmann, T., Boone, C. D., Elkins, J. W., Engel, A., Glatthor, N., Grabowski, U., Harth, C. M., Kiefer, M., Kolonjari, F., Krummel, P. B., Linden, A., Lunder, C. R., Miller, B. R., Montzka, S. A., Mühle, J., O'Doherty, S., Orphal, J., Prinn, R. G., Toon, G., Vollmer, M. K., Walker, K. A., Weiss, R. F., Wiecele, A., and Young, D.: Global HCFC-22 measurements with MIPAS:
565 retrieval, validation, global distribution and its evolution over 2005–2012, *Atmos. Chem. Phys.*, 16, 3345–3368, <https://doi.org/10.5194/acp-16-3345-2016>, 2016.
- Clarmann, T. von and Johansson, S.: Chlorine nitrate in the atmosphere, *Atmos. Chem. Phys.*, 18, 15363–15386, <https://doi.org/10.5194/acp-18-15363-2018>, 2018.
- Cortesi, U., Lambert, J. C., Clercq, C. de, Bianchini, G., Blumenstock, T., Bracher, A.,
570 Castelli, E., Catoire, V., Chance, K. V., Mazière, M. de, Demoulin, P., Godin-Beekmann,



- S., Jones, N., Jucks, K., Keim, C., Kerzenmacher, T., Kuellmann, H., Kuttippurath, J., Iarlori, M., Liu, G. Y., Liu, Y., McDermid, I. S., Meijer, Y. J., Mencaraglia, F., Mikuteit, S., Oelhaf, H., Piccolo, C., Pirre, M., Raspollini, P., Ravegnani, F., Reburn, W. J., Redaelli, G., Remedios, J. J., Sembhi, H., Smale, D., Steck, T., Taddei, A., Varotsos, C.,
575 Vigouroux, C., Waterfall, A., Wetzol, G., and Wood, S.: Geophysical validation of MIPAS-ENVISAT operational ozone data, *Atmos. Chem. Phys.*, 7, 4807–4867, <https://doi.org/10.5194/acp-7-4807-2007>, 2007.
- Crutzen, P. J.: The possible importance of CSO for the sulfate layer of the stratosphere, *Geophys. Res. Lett.*, 3, 73–76, <https://doi.org/10.1029/GL003i002p00073>, 1976.
- 580 Dessler, A. E., Schoeberl, M. R., Wang, T., Davis, S. M., Rosenlof, K. H., and Vernier, J.-P.: Variations of stratospheric water vapor over the past three decades, *J. Geophys. Res. Atmos.*, 119, 12,588–12,598, <https://doi.org/10.1002/2014JD021712>, 2014.
- Dhomse, S. S., Feng, W., Montzka, S. A., Hossaini, R., Keeble, J., Pyle, J. A., Daniel, J. S., and Chipperfield, M. P.: Delay in recovery of the Antarctic ozone hole from unexpected
585 CFC-11 emissions, *Nature Communications*, 10, 5781, <https://doi.org/10.1038/s41467-019-13717-x>, 2019.
- Dinelli, B. M., Raspollini, P., Gai, M., Sgheri, L., Ridolfi, M., Ceccherini, S., Barbara, F., Zoppetti, N., Castelli, E., Papandrea, E., Pettinari, P., Dehn, A., Dudhia, A., Kiefer, M., Piro, A., Flaud, J.-M., López-Puertas, M., Moore, D., Remedios, J., and Bianchini, M.:
590 The ESA MIPAS/Envisat level2-v8 dataset: 10 years of measurements retrieved with ORM v8.22, *Atmos. Meas. Tech.*, 14, 7975–7998, <https://doi.org/10.5194/amt-14-7975-2021>, 2021.
- Dudhia, A., Jay, V. L., and Rodgers, C. D.: Microwindow selection for high-spectral-resolution sounders, *Appl. Opt.*, 41, 3665, <https://doi.org/10.1364/AO.41.003665>, 2002.
- 595 Engel, A., Bönisch, H., Schwarzenberger, T., Haase, H.-P., Grunow, K., Abalichin, J., and Sala, S.: Long-term validation of ESA operational retrieval (version 6.0) of MIPAS Envisat vertical profiles of methane, nitrous oxide, CFC11, and CFC12 using balloon-borne observations and trajectory matching, *Atmos. Meas. Tech.*, 9, 1051–1062, <https://doi.org/10.5194/amt-9-1051-2016>, 2016.



- 600 ESA: New Envisat MIPAS L2 dataset reprocessed with ORM v822 available - Earth Online,
available at: <https://earth.esa.int/eogateway/news/new-envisat-mipas-l2-dataset-reprocessed-with-orm-v822-available> (last access: 12 July 2022), 2021.
- ESA: ESA declares end of mission for Envisat, available at:
https://www.esa.int/Applications/Observing_the_Earth/Envisat/ESA_declares_end_of_mission_for_Envisat (last access: 12 July 2022), 2012.
- 605
- Fischer, H., Birk, M., Blom, C., Carli, B., Carlotti, M., Clarmann, T. von, Delbouille, L.,
Dudhia, A., Ehhalt, D., Endemann, M., Flaud, J. M., Gessner, R., Kleinert, A., Koopman,
R., Langen, J., López-Puertas, M., Mosner, P., Nett, H., Oelhaf, H., Perron, G., Remedios,
J., Ridolfi, M., Stiller, G., and Zander, R.: MIPAS: an instrument for atmospheric and
610 climate research, *Atmos. Chem. Phys.*, 8, 2151–2188, <https://doi.org/10.5194/acp-8-2151-2008>, 2008.
- Friedl-Vallon, F., Maucher, G., Seefeldner, M., Trieschmann, O., Kleinert, A., Lengel, A.,
Keim, C., Oelhaf, H., and Fischer, H.: Design and characterization of the balloon-borne
Michelson Interferometer for Passive Atmospheric Sounding (MIPAS-B2), *Appl. Opt.*,
615 43, 3335, <https://doi.org/10.1364/AO.43.003335>, 2004.
- Fu, D., Boone, C. D., Bernath, P. F., Walker, K. A., Nassar, R., Manney, G. L., and McLeod,
S. D.: Global phosgene observations from the Atmospheric Chemistry Experiment (ACE)
mission, *Geophys. Res. Lett.*, 34, 32, <https://doi.org/10.1029/2007GL029942>, 2007.
- Glatthor, N., Clarmann, T. von, Stiller, G. P., Funke, B., Koukouli, M. E., Fischer, H.,
620 Grabowski, U., Höpfner, M., Kellmann, S., and Linden, A.: Large-scale upper
tropospheric pollution observed by MIPAS HCN and C₂H₆ global distributions, *Atmos.
Chem. Phys.*, 9, 9619–9634, <https://doi.org/10.5194/acp-9-9619-2009>, 2009.
- Glatthor, N., Höpfner, M., Leyser, A., Stiller, G. P., Clarmann, T. von, Grabowski, U.,
Kellmann, S., Linden, A., Sinnhuber, B.-M., Krysztofiak, G., and Walker, K. A.: Global
625 carbonyl sulfide (OCS) measured by MIPAS/Envisat during 2002–2012, *Atmos. Chem.
Phys.*, 17, 2631–2652, <https://doi.org/10.5194/acp-17-2631-2017>, 2017.
- Grunow, K.: Anwendung von Trajektorien zur ENVISAT-Validierung und zur Untersuchung
der Luftmassenherkunft in der Stratosphäre, PhD, Free University Berlin, Berlin,
Germany, 2009.



- 630 Harrison, J. J.: New and improved infrared absorption cross sections for
dichlorodifluoromethane (CFC-12), *Atmos. Meas. Tech.*, 8, 3197–3207,
<https://doi.org/10.5194/amt-8-3197-2015>, 2015.
- Harrison, J. J., Chipperfield, M. P., Dudhia, A., Cai, S., Dhomse, S., Boone, C. D., and
Bernath, P. F.: Satellite observations of stratospheric carbonyl fluoride, *Atmos. Chem.*
635 *Phys.*, 14, 11915–11933, <https://doi.org/10.5194/acp-14-11915-2014>, 2014.
- Harrison, J. J.: New and improved infrared absorption cross sections for
chlorodifluoromethane (HCFC-22), *Atmos. Meas. Tech.*, 9, 2593–2601,
<https://doi.org/10.5194/amt-9-2593-2016>, 2016.
- Harrison, J. J., Boone, C. D., and Bernath, P. F.: New and improved infra-red absorption cross
640 sections and ACE-FTS retrievals of carbon tetrachloride (CCl₄), *Journal of Quantitative
Spectroscopy and Radiative Transfer*, 186, 139–149,
<https://doi.org/10.1016/j.jqsrt.2016.04.025>, 2017.
- Hegglin, M. I., Tegtmeier, S., Anderson, J., Bourassa, A. E., Brohede, S., Degenstein, D.,
Froidevaux, L., Funke, B., Gille, J., Kasai, Y., Kyrölä, E. T., Lumpe, J., Murtagh, D., Neu,
645 J. L., Pérot, K., Remsberg, E. E., Rozanov, A., Toohey, M., Urban, J., Clarmann, T. von,
Walker, K. A., Wang, H.-J., Arosio, C., Damadeo, R., Fuller, R. A., Lingenfelter, G.,
McLinden, C., Pendlebury, D., Roth, C., Ryan, N. J., Sioris, C., Smith, L., and Weigel, K.:
Overview and update of the SPARC Data Initiative: comparison of stratospheric
composition measurements from satellite limb sounders, *Earth Syst. Sci. Data*, 13, 1855–
650 1903, <https://doi.org/10.5194/essd-13-1855-2021>, 2021.
- Höpfner, M., Oelhaf, H., Wetzell, G., Friedl-Vallon, F., Kleinert, A., Lengel, A., Maucher, G.,
Nordmeyer, H., Glatthor, N., Stiller, G., Clarmann, T. v., Fischer, H., Kröger, C., and
Deshler, T.: Evidence of scattering of tropospheric radiation by PSCs in mid-IR limb
emission spectra: MIPAS-B observations and KOPRA simulations, *Geophys. Res. Lett.*,
655 29, 119-1-119-4, <https://doi.org/10.1029/2001GL014443>, 2002.
- Hubert, D., Keppens, A., Granville, J., and Lambert, J.-C.: Validation report: comparison of
MIPAS ORM 8.22 to ground-based data TN-BIRA-IASB-MultiTASTE-Phase-F-MIPAS-
ORM8-Iss1-RevB, available at:
[https://earth.esa.int/eogateway/documents/20142/37627/TN-BIRA-IASB-MultiTASTE-
660 Phase-F-MIPAS-ORM8-Iss1-RevB.pdf](https://earth.esa.int/eogateway/documents/20142/37627/TN-BIRA-IASB-MultiTASTE-Phase-F-MIPAS-ORM8-Iss1-RevB.pdf) (last access: 12 July 2022), 2020.



- 665 Khosrawi, F., Lossow, S., Stiller, G. P., Rosenlof, K. H., Urban, J., Burrows, J. P., Damadeo,
R. P., Eriksson, P., García-Comas, M., Gille, J. C., Kasai, Y., Kiefer, M., Nedoluha, G. E.,
Noël, S., Raspollini, P., Read, W. G., Rozanov, A., Sioris, C. E., Walker, K. A., and
Weigel, K.: The SPARC water vapour assessment II: comparison of stratospheric and
lower mesospheric water vapour time series observed from satellites, *Atmos. Meas. Tech.*,
11, 4435–4463, <https://doi.org/10.5194/amt-11-4435-2018>, 2018.
- 670 Kindler, T. P., Chameides, W. L., Wine, P. H., Cunnold, D. M., Alyea, F. N., and Franklin, J.
A.: The fate of atmospheric phosgene and the stratospheric chlorine loadings of its parent
compounds: CCl₄, C₂Cl₄, C₂HCl₃, CH₃CCl₃, and CHCl₃, *J. Geophys. Res.*, 100, 1235–
1251, <https://doi.org/10.1029/94JD02518>, 1995.
- Ko, M. K. W. and Dak Sze, N.: A 2-D model calculation of atmospheric lifetimes for N₂O,
CFC-11 and CFC-12, *Nature*, 297, 317–319, <https://doi.org/10.1038/297317a0>, 1982.
- 675 Kremser, S., Thomason, L. W., Hobe, M. von, Hermann, M., Deshler, T., Timmreck, C.,
Toohey, M., Stenke, A., Schwarz, J. P., Weigel, R., Fueglistaler, S., Prata, F. J., Vernier,
J.-P., Schlager, H., Barnes, J. E., Antuña-Marrero, J.-C., Fairlie, D., Palm, M., Mahieu, E.,
Notholt, J., Rex, M., Bingen, C., Vanhellemont, F., Bourassa, A., Plane, J. M. C., Klocke,
D., Carn, S. A., Clarisse, L., Trickl, T., Neely, R., James, A. D., Rieger, L., Wilson, J. C.,
and Meland, B.: Stratospheric aerosol-Observations, processes, and impact on climate,
Rev. Geophys., 54, 278–335, <https://doi.org/10.1002/2015RG000511>, 2016.
- 680 Li, Q., Jacob, D. J., Yantosca, R. M., Heald, C. L., Singh, H. B., Koike, M., Zhao, Y., Sachse,
G. W., and Streets, D. G.: A global three-dimensional model analysis of the atmospheric
budgets of HCN and CH₃CN: Constraints from aircraft and ground measurements, *J.
Geophys. Res.*, 108, 955, <https://doi.org/10.1029/2002JD003075>, 2003.
- 685 Lossow, S., Hurst, D. F., Rosenlof, K. H., Stiller, G. P., Clarmann, T. von, Brinkop, S.,
Dameris, M., Jöckel, P., Kinnison, D. E., Plieninger, J., Plummer, D. A., Ploeger, F.,
Read, W. G., Remsberg, E. E., Russell, J. M., and Tao, M.: Trend differences in lower
stratospheric water vapour between Boulder and the zonal mean and their role in
understanding fundamental observational discrepancies, *Atmos. Chem. Phys.*, 18, 8331–
8351, <https://doi.org/10.5194/acp-18-8331-2018>, 2018.



- 690 Michelsen, H. A., Manney, G. L., Gunson, M. R., and Zander, R.: Correlations of stratospheric abundances of NO_y, O₃, N₂O, and CH₄ derived from ATMOS measurements, *J. Geophys. Res. Atmos.*, 103, 28347–28359, <https://doi.org/10.1029/98JD02850>, 1998.
- Naujokat, B. and Grunow, K.: The stratospheric Arctic winter 2002/03: Balloon flight planning by trajectory calculations, 16th Esa Symposium on European Rocket and Balloon Programmes and Related Research, Proceedings, 530, 421–425, 2003.
- 695 Parker, R. J., Remedios, J. J., Moore, D. P., and Kanawade, V. P.: Acetylene C₂H₂ retrievals from MIPAS data and regions of enhanced upper tropospheric concentrations in August 2003, *Atmos. Chem. Phys.*, 11, 10243–10257, <https://doi.org/10.5194/acp-11-10243-2011>, 2011.
- 700 Payan, S., Camy-Peyret, C., Oelhaf, H., Wetzel, G., Maucher, G., Keim, C., Pirre, M., Huret, N., Engel, A., Volk, M. C., Kuellmann, H., Kuttippurath, J., Cortesi, U., Bianchini, G., Mencaraglia, F., Raspollini, P., Redaelli, G., Vigouroux, C., Mazière, M. de, Mikuteit, S., Blumenstock, T., Velazco, V., Notholt, J., Mahieu, E., Duchatelet, P., Smale, D., Wood, S., Jones, N., Piccolo, C., Payne, V., Bracher, A., Glatthor, N., Stiller, G., Grunow, K.,
- 705 Jeseck, P., Te, Y., and Butz, A.: Validation of version-4.61 methane and nitrous oxide observed by MIPAS, *Atmos. Chem. Phys.*, 9, 413–442, <https://doi.org/10.5194/acp-9-413-2009>, 2009.
- Pettinari, P., Barbara, F., Ceccherini, S., Dinelli, B. M., Gai, M., Raspollini, P., Sgheri, L., Valeri, M., Wetzel, G., Zoppetti, N., and Ridolfi, M.: Phosgene distribution derived from MIPAS ESA v8 data: intercomparisons and trends, *Atmos. Meas. Tech.*, 14, 7959–7974, <https://doi.org/10.5194/amt-14-7959-2021>, 2021.
- 710 Phillips, D. L.: A technique for the numerical solution of certain integral equations of the first kind, *J. Assoc. Comput. Math.*, 9, 84–97, <https://doi.org/10.1145/321105.321114>, 1962.
- Prinn, R. G., Weiss, R. F., Fraser, P. J., Simmonds, P. G., Cunnold, D. M., Alyea, F. N.,
- 715 O'Doherty, S., Salameh, P., Miller, B. R., Huang, J., Wang, R. H. J., Hartley, D. E., Harth, C., Steele, L. P., Sturrock, G., Midgley, P. M., and McCulloch, A.: A history of chemically and radiatively important gases in air deduced from ALE/GAGE/AGAGE, *J. Geophys. Res.*, 105, 17751–17792, <https://doi.org/10.1029/2000JD900141>, 2000.
- Raspollini, P., Arnone, E., Barbara, F., Bianchini, M., Carli, B., Ceccherini, S., Chipperfield, M. P., Dehn, A., Della Fera, S., Dinelli, B. M., Dudhia, A., Flaud, J.-M., Gai, M., Kiefer,
- 720



- M., López-Puertas, M., Moore, D. P., Piro, A., Remedios, J. J., Ridolfi, M., Sembhi, H., Sgheri, L., and Zoppetti, N.: Level 2 processor and auxiliary data for ESA Version 8 final full mission analysis of MIPAS measurements on ENVISAT, *Atmos. Meas. Tech.*, 15, 1871–1901, <https://doi.org/10.5194/amt-15-1871-2022>, 2022.
- 725 Raspollini, P., Piro, A., Hubert, D., Keppens, A., Lambert, J.-C., Wetzels, G., Moore, D., Ceccherini, S., Gai, M., Barbara, F., and Zoppetti, N.: Environmental Satellite (ENVISAT) Michelson Interferometer for Passive Atmospheric Sounding (MIPAS), ESA Level 2 version 8.22 products - product quality readme file, available at: https://earth.esa.int/eogateway/documents/20142/37627/README_V8_issue_1.0_20201221.pdf (last access: 12 July 2022), 2020.
- 730 Raspollini, P., Carli, B., Carlotti, M., Ceccherini, S., Dehn, A., Dinelli, B. M., Dudhia, A., Flaud, J.-M., López-Puertas, M., Niro, F., Remedios, J. J., Ridolfi, M., Sembhi, H., Sgheri, L., and Clarmann, T. von: Ten years of MIPAS measurements with ESA Level 2 processor V6 – Part 1: Retrieval algorithm and diagnostics of the products, *Atmos. Meas. Tech.*, 6, 2419–2439, <https://doi.org/10.5194/amt-6-2419-2013>, 2013.
- 735 Raspollini, P., Belotti, C., Burgess, A., Carli, B., Carlotti, M., Ceccherini, S., Dinelli, B. M., Dudhia, A., Flaud, J.-M., Funke, B., Höpfner, M., Lopez-Puertas, M., Payne, V., Piccolo, C., Remedios, J. J., Ridolfi, M., and Spang, R.: MIPAS level 2 operational analysis, *Atmos. Chem. Phys.*, 6, 5605–5630, <https://doi.org/10.5194/acp-6-5605-2006>, 2006.
- 740 Ridolfi, M., Blum, U., Carli, B., Catoire, V., Ceccherini, S., Claude, H., Clercq, C. de, Fricke, K. H., Friedl-Vallon, F., Iarlori, M., Keckhut, P., Kerridge, B., Lambert, J.-C., Meijer, Y. J., Mona, L., Oelhaf, H., Pappalardo, G., Pirre, M., Rizi, V., Robert, C., Swart, D., Clarmann, T. von, Waterfall, A., and Wetzels, G.: Geophysical validation of temperature retrieved by the ESA processor from MIPAS/ENVISAT atmospheric limb-emission measurements, *Atmos. Chem. Phys.*, 7, 4459–4487, <https://doi.org/10.5194/acp-7-4459-2007>, 2007.
- 745 Ridolfi, M., Carli, B., Carlotti, M., Clarmann, T. von, Dinelli, B. M., Dudhia, A., Flaud, J.-M., Höpfner, M., Morris, P. E., Raspollini, P., Stiller, G., and Wells, R. J.: Optimized forward model and retrieval scheme for MIPAS near-real-time data processing, *Appl. Opt.*, 39, 1323, <https://doi.org/10.1364/AO.39.001323>, 2000.
- 750 Rodgers, C. D.: *Inverse methods for atmospheric sounding*, 2, World Sci., 2000.



- Rothman, L. S., Gordon, I. E., Barbe, A., Benner, D., Bernath, P. F., Birk, M., Boudon, V.,
Brown, L. R., Campargue, A., Champion, J.-P., Chance, K., Coudert, L. H., Dana, V.,
Devi, V. M., Fally, S., Flaud, J.-M., Gamache, R. R., Goldman, A., Jacquemart, D.,
755 Kleiner, I., Lacombe, N., Lafferty, W. J., Mandin, J.-Y., Massie, S. T., Mikhailenko, S. N.,
Miller, C. E., Moazzen-Ahmadi, N., Naumenko, O. V., Nikitin, A. V., Orphal, J.,
Perevalov, V. I., Perrin, A., Predoi-Cross, A., Rinsland, C. P., Rotger, M., Šimečková, M.,
Smith, M., Sung, K., Tashkun, S. A., Tennyson, J., Toth, R. A., Vandaele, A. C., and
Vander Auwera, J.: The HITRAN 2008 molecular spectroscopic database, *Journal of*
760 *Quantitative Spectroscopy and Radiative Transfer*, 110, 533–572,
<https://doi.org/10.1016/j.jqsrt.2009.02.013>, 2009.
- Rudolph, J.: The tropospheric distribution and budget of ethane, *J. Geophys. Res.*, 100,
11369, <https://doi.org/10.1029/95JD00693>, 1995.
- Singh, H. B., Herlth, D., Kolyer, R., Chatfield, R., Viezee, W., Salas, L. J., Chen, Y.,
765 Bradshaw, J. D., Sandholm, S. T., Talbot, R., Gregory, G. L., Anderson, B., Sachse, G.
W., Browell, E., Bachmeier, A. S., Blake, D. R., Heikes, B., Jacob, D., and Fuelberg, H.
E.: Impact of biomass burning emissions on the composition of the South Atlantic
troposphere: Reactive nitrogen and ozone, *J. Geophys. Res.*, 101, 24203–24219,
<https://doi.org/10.1029/96JD01018>, 1996.
- 770 Sinnhuber, M., Burrows, J. P., Chipperfield, M. P., Jackman, C. H., Kallenrode, M.-B.,
Künzi, K. F., and Quack, M.: A model study of the impact of magnetic field structure on
atmospheric composition during solar proton events, *Geophys. Res. Lett.*, 30, 1781,
<https://doi.org/10.1029/2003GL017265>, 2003.
- Stiller, G. P., Clarmann, T. von, Funke, B., Glatthor, N., Hase, F., Höpfner, M., and Linden,
775 A.: Sensitivity of trace gas abundances retrievals from infrared limb emission spectra to
simplifying approximations in radiative transfer modelling, *Journal of Quantitative*
Spectroscopy and Radiative Transfer, 72, 249–280, [https://doi.org/10.1016/S0022-](https://doi.org/10.1016/S0022-4073(01)00123-6)
4073(01)00123-6, 2002.
- Tchana, F. K., Lafferty, W. J., Flaud, J.-M., Manceron, L., and Ndao, M.: High-resolution
780 analysis of the ν_1 and ν_5 bands of phosgene $^{35}\text{Cl}_2\text{CO}$ and $^{35}\text{Cl}^{37}\text{ClCO}$, *Molecular Physics*,
113, 3241–3246, <https://doi.org/10.1080/00268976.2015.1015638>, 2015.



- Tikhonov, A. N.: On the solution of ill-posed problems and the method of regularization, Dokl. Acad. Nauk SSSR, 151, 501–504, 1963.
- Toon, G. C., Blavier, J.-F., Sen, B., and Drouin, B. J.: Atmospheric COCl₂ measured by solar occultation spectrometry, Geophys. Res. Lett., 28, 2835–2838, 785
<https://doi.org/10.1029/2000GL012156>, 2001.
- Valeri, M., Barbara, F., Boone, C., Ceccherini, S., Gai, M., Maucher, G., Raspollini, P., Ridolfi, M., Sgheri, L., Wetzel, G., and Zoppetti, N.: CCl₄ distribution derived from MIPAS ESA v7 data: intercomparisons, trend, and lifetime estimation, Atmos. Chem. Phys., 17, 10143–10162, 790
<https://doi.org/10.5194/acp-17-10143-2017>, 2017.
- Valeri, M., Carlotti, M., Flaud, J.-M., Raspollini, P., Ridolfi, M., and Dinelli, B. M.: Phosgene in the UTLS: seasonal and latitudinal variations from MIPAS observations, Atmos. Meas. Tech., 9, 4655–4663, <https://doi.org/10.5194/amt-9-4655-2016>, 2016.
- Wang, D. Y., Höpfner, M., Blom, C. E., Ward, W. E., Fischer, H., Blumenstock, T., Hase, F., Keim, C., Liu, G. Y., Mikuteit, S., Oelhaf, H., Wetzel, G., Cortesi, U., Mencaraglia, F., Bianchini, G., Redaelli, G., Pirre, M., Catoire, V., Huret, N., Vigouroux, C., Mazière, M. de, Mahieu, E., Demoulin, P., Wood, S., Smale, D., Jones, N., Nakajima, H., Sugita, T., Urban, J., Murtagh, D., Boone, C. D., Bernath, P. F., Walker, K. A., Kuttippurath, J., Kleinböhl, A., Toon, G., and Piccolo, C.: Validation of MIPAS HNO₃ operational data, 795
Atmos. Chem. Phys., 7, 4905–4934, <https://doi.org/10.5194/acp-7-4905-2007>, 2007.
- Wetzel, G., Höpfner, M., and Oelhaf, H.: CCN #2: Support to MIPAS level 2 processor verification and validation - Phase F: Report to MS6_2: L1v8/L2v8 FM comparison for GL1-GL3; Long-term validation of MIPAS ESA operational products using MIPAS-B measurements, available at: 805
https://earth.esa.int/eogateway/documents/20142/37627/kit_ccn_2_esa_tn-fr_2020_01.pdf (last access: 12 July 2022), 2020.
- Wetzel, G., Oelhaf, H., Birk, M., Lange, A. de, Engel, A., Friedl-Vallon, F., Kirner, O., Kleinert, A., Maucher, G., Nordmeyer, H., Orphal, J., Ruhnke, R., Sinnhuber, B.-M., and Vogt, P.: Partitioning and budget of inorganic and organic chlorine species observed by MIPAS-B and TELIS in the Arctic in March 2011, Atmos. Chem. Phys., 15, 8065–8076, 810
<https://doi.org/10.5194/acp-15-8065-2015>, 2015.



- Wetzel, G., Oelhaf, H., Berthet, G., Bracher, A., Cornacchia, C., Feist, D. G., Fischer, H., Fix, A., Iarlori, M., Kleinert, A., Lengel, A., Milz, M., Mona, L., Müller, S. C., Ovarlez, J., Pappalardo, G., Piccolo, C., Raspollini, P., Renard, J.-B., Rizi, V., Rohs, S., Schiller, C.,
815 Stiller, G., Weber, M., and Zhang, G.: Validation of MIPAS-ENVISAT H₂O operational data collected between July 2002 and March 2004, *Atmos. Chem. Phys.*, 13, 5791–5811, <https://doi.org/10.5194/acp-13-5791-2013>, 2013a.
- Wetzel, G., Oelhaf, H., Friedl-Vallon, F., Kleinert, A., Maucher, G., Nordmeyer, H., and Orphal, J.: Long-term intercomparison of MIPAS additional species ClONO₂, N₂O₅, CFC-11, and CFC-12 with MIPAS-B measurements, *Annals of Geophysics*, 56,
820 <https://doi.org/10.4401/ag-6329>, 2013b.
- Wetzel, G., Oelhaf, H., Kirner, O., Friedl-Vallon, F., Ruhnke, R., Ebersoldt, A., Kleinert, A., Maucher, G., Nordmeyer, H., and Orphal, J.: Diurnal variations of reactive chlorine and nitrogen oxides observed by MIPAS-B inside the January 2010 Arctic vortex, *Atmos. Chem. Phys.*, 12, 6581–6592, <https://doi.org/10.5194/acp-12-6581-2012>, 2012.
825
- Wetzel, G., Oelhaf, H., Kirner, O., Ruhnke, R., Friedl-Vallon, F., Kleinert, A., Maucher, G., Fischer, H., Birk, M., Wagner, G., and Engel, A.: First remote sensing measurements of ClOOCl along with ClO and ClONO₂ in activated and deactivated Arctic vortex conditions using new ClOOCl IR absorption cross sections, *Atmos. Chem. Phys.*, 10, 931–945, <https://doi.org/10.5194/acp-10-931-2010>, 2010.
830
- Wetzel, G., Bracher, A., Funke, B., Goutail, F., Hendrick, F., Lambert, J.-C., Mikuteit, S., Piccolo, C., Pirre, M., Bazureau, A., Belotti, C., Blumenstock, T., Mazière, M. de, Fischer, H., Huret, N., Ionov, D., López-Puertas, M., Maucher, G., Oelhaf, H., Pommereau, J.-P., Ruhnke, R., Sinnhuber, M., Stiller, G., van Roozendaal, M., and Zhang, G.: Validation of
835 MIPAS-ENVISAT NO₂ operational data, *Atmos. Chem. Phys.*, 7, 3261–3284, <https://doi.org/10.5194/acp-7-3261-2007>, 2007.
- Wiegele, A., Glatthor, N., Höpfner, M., Grabowski, U., Kellmann, S., Linden, A., Stiller, G., and Clarmann, T. von: Global distributions of C₂H₆, C₂H₂, HCN, and PAN retrieved from MIPAS reduced spectral resolution measurements, *Atmos. Meas. Tech.*, 5, 723–734,
840 <https://doi.org/10.5194/amt-5-723-2012>, 2012.



Xiao, Y., Logan, J. A., Jacob, D. J., Hudman, R. C., Yantosca, R., and Blake, D. R.: Global budget of ethane and regional constraints on U.S. sources, *J. Geophys. Res.*, 113, 955, <https://doi.org/10.1029/2007JD009415>, 2008.

845 Yokouchi, Y., Noijiri, Y., Barrie, L. A., Toom-Sauntry, D., Machida, T., Inuzuka, Y., Akimoto, H., Li, H. J., Fujinuma, Y., and Aoki, S.: A strong source of methyl chloride to the atmosphere from tropical coastal land, *Nature*, 403, 295–298, <https://doi.org/10.1038/35002049>, 2000.